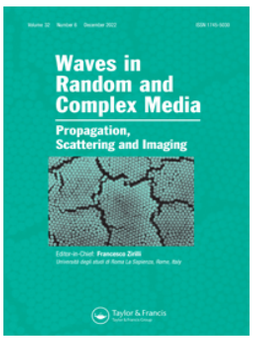

Waves in Random and Complex Media

ISSN: (Print) (Online) Journal homepage: https://www.tandfonline.com/loi/twrm20

Impact of thermal radiation and oriented magnetic field on the flow of two immiscible fluids through porous media with different porosity

Pramod Kumar Yadav, Ankit Kumar, Shreen El-Sapa & Ali J. Chamkha

To cite this article: Pramod Kumar Yadav, Ankit Kumar, Shreen El-Sapa & Ali J. Chamkha (2022): Impact of thermal radiation and oriented magnetic field on the flow of two immiscible fluids through porous media with different porosity, Waves in Random and Complex Media, DOI: 10.1080/17455030.2022.2118897

To link to this article: https://doi.org/10.1080/17455030.2022.2118897

Published online: 14 Sep 2022.

WAVES IN RANDOM AND COMPLEX MEDIA
https://doi.org/10.1080/17455030.2022.2118897

Taylor & Francis
Taylor & Francis Group

Check for updates

Impact of thermal radiation and oriented magnetic field on the flow of two immiscible fluids through porous media with different porosity

Pramod Kumar Yadav [1], Ankit Kumar[1], Shreen El-Sapa[2] and Ali J. Chamkha[3]

[1]Department of Mathematics, Motilal Nehru National Institute of Technology Allahabad, Prayagraj, India; [2]Department of Mathematics, College of Science, Princess Nourah Bint Abdulrahman University, Riyadh, Saudi Arabia; [3]Faculty of Engineering, Kuwait College of Science and Technology, Doha District, Kuwait

ABSTRACT

This work analyzes the impact of oriented magnetic fields and thermal radiation on the entropy generation of two non-miscible electrically conducting micropolar and Newtonian fluids in a horizontal rectangular porous channel. In this model, the walls of the duct are considered perfectly isothermal and the flow inside the porous channel takes place in the presence of an inclined magnetic field. Expressions for heat transformation, fluid flow velocity, Bejan number distribution, and entropy production characteristics are obtained with the help of a reliable method. To achieve the objective of the problem, the authors used the continuity of temperature distribution, thermal flux, shear stress, linear and angular velocity over the fluid–fluid interface and no-slip conditions at the fixed plates of the duct. The impact of various emerging parameters on the entropy optimization, Bejan number, heat transformation, and flow velocity is analyzed. Our findings are validated by the previously established results.

ARTICLE HISTORY
Received 29 May 2022
Accepted 23 August 2022

KEYWORDS
Micropolar fluid; immiscible fluid; thermal radiation; oriented magnetic field; porous media; entropy optimization

1. Introduction

The flow of immiscible Newtonian and non-Newtonian fluids has a number of real-life applications in chemical engineering, manufacturing processes, cosmetic industries, pharmaceutical processes, etc. Non-Newtonian fluids have complex physical and rheological properties that cannot be studied by the classical Navier–Stokes formulation. These fluids are categorized by the class of non-Newtonian fluid mechanics. A number of researchers have worked on non-Newtonian fluids and addressed various non-Newtonian fluid models such as Jeffrey fluid, Reiner–Rivlin fluids, micropolar fluid, power-law fluid, Maxwell and Oldroyd-B fluids, couple stress fluid, second, third, and fourth-grade fluids, Casson fluid, and so on. Micropolar fluids are an important class of non-Newtonian fluids whose behavior matches with the various real-life fluids. Micropolar fluid particles possess the micro-rotational inertia and micro-rotational effects. The theory of micropolar fluid developed by

CONTACT Pramod Kumar Yadav pramodky@mnnit.ac.in

Eringen [1,2] provided new dimensions of research for the researchers and scientist. Ariman et al. [3,4] presented a comprehensive review of microcontinuum field theories and provided distinct applications in ideal and real fluid flow problems. Lukaszewicz [5] also did work on micropolar fluid theory and presented its enormous applications in real life. Later on, a number of researchers used the theory of micropolar fluid to develop various models for real-life problems. Yadav and Verma [6] discussed a model of non-miscible fluids flow through a cylindrical channel which is bounded by a porous cylinder. Khanukaeva et al. [7] discussed the flow behavior of micropolar fluid through a porous layered membrane using cell model technique. In this work, they analyzed the influence of porosity parameter and micropolarity parameter on hydrodynamic permeability of a membrane. Oahimire and Olajuwon [8] estimated the mass exchange and heat transfer of unsteady, incompressible, magnetohydrodynamic, and chemically reacting flow regimes of micropolar fluid inside a vertical porous conduit. In this work, they used perturbation technique to evaluate flow velocity, temperature profile, microrotation, and concentration. Srinivasacharya and Bindu [9] examined the production of entropy in an inclined conduit due to the flow of micropolar fluid with a constant pressure gradient and convective boundary conditions. They utilized spectral quasilinearization technique to find the expressions for temperature profiles, microrotation and flow velocity. Ahmed and Rashad [10] studied the thermal exchange and convective flow of micropolar nanofluid within a rectangular porous enclosure. They solved the governing system of equations numerically by using the finite volume method with SIMPLE technique. Jena and Mathur [11] discussed the boundary layer and convective flow of micropolar fluid past a vertical flat plate. Bhattacharya et al. [12] discussed the impact of radiative heat transfer on the micropolar fluid flow through a porous shrinking sheet.

The subject of MHD flow and heat transformation is generating considerable interest among researchers and scientists in terms of MHD accelerators and generators, MHD heat pumps, energy storage, geophysics etc. Yadav and Jaiswal [13] examined the two-phase non-miscible fluid layers of micropolar and Newtonian fluid inside a horizontal porous conduit in the presence of an oriented magnetic field. In this work, they showed that how the oriented magnetic field can be used to control the flow velocity of inside the porous channel. Nikodijevic et al. [14] presented a MHD Couette flow model of non-miscible Newtonian viscous fluids in a static horizontal duct with the influence of oriented magnetic and applied electric fields. Srivastava and Deo [15] worked on electrically conducting, fully developed, incompressible viscous fluids in a porous saturated medium under the action of variable permeability and transverse magnetic field. They used the Brinkman equation for the modeling of fluid through porous medium. Komurgoz et al. [16] analyzed the impact of magnetic field on the entropy production and heat transfer for incompressible and laminar flow of fluid through a porous saturated inclined channel. The major advantages of this work are to give open-form solution by using generalized differential quadrature method (GDQM) and differential transform method (DTM). Sharma and Yadav [17] discussed the magnetic field effect on two-phase flow of blood through narrow blood vessels. Bhatti and Abdelsalam [18] analyzed the impact of an applied and induced magnetic field on the peristaltically driven flow of Carreau fluid in a symmetric channel. Shahid et al. [19] examined the chemical reaction and activation energy on bi-convection flow of MHD Carreau nanofluid past an upper paraboloid porous saturated surface. Bhatti et al. [20] numerically investigated the impact of thermal radiation on MHD flow of Carreau nanofluid over a shrinking sheet.

Rashidi et al. [21] described the entropy production during the peristaltic blood like-flow of MHD nanofluid in an asymmetric channel.

The flow of fluid through various media and materials such as sponges, earth's surfaces, branches of plants and reservoir rocks motivated us to study the flow of fluid through porous materials. The flow equation which governs the flow of fluid through porous substances is suggested by Darcy [22]. Darcy's formulation is defined for low permeability porous material. Brinkman [23] estimated the viscous force developed from flowing fluid in a dense swarm of particles and introduced the modified Darcy's equation, which is also known as Brinkman equation. For high porosity medium, the equation suggested by Brinkman [23] is more appropriate as compared to Darcy model. The comprehensive literature on the subject of free and forced convection through porous media is well described by Bejan [24] and Nield and Bejan [25]. Vafai and Tien [26] studied the nature of inertial and boundary effects upon thermal exchange and fluid flow in porous media. Kaviany [27] expressed analytical and theoretical solutions for the Darcy–Brinkman model. Rudraiah and Nagaraj [28] estimated the impact of viscous dissipation as well as Darcy parameter on natural convective and fully developed flow of fluid within a heated vertical porous stratum. In this work, they concluded that the obtained results may be useful in plant physiology by proper adjustment of temperature distribution. Kaviany [29] considered the laminar fluid flow regime within a porous medium sandwiched by isothermal parallel plates. Umavathi et al. [30] studied the unsteady fluid flow and heat transformation of viscous fluid through a horizontal rectangular porous enclosure. They used recognized model of Darcy–Brinkman to formulate the fluid flow problem. Chamkha [31] analyzed the hydromagnetic, steady, laminar flow regime, and thermal characteristics of non-miscible fluid in a vertical non-porous and porous conduit and concluded that obtained results may be useful in coal-fired MHD generators, in filtration system and oil recovery system where the porous medium is present. Morosuk [32] investigates entropy production due to laminar flows in an isothermal partially or fully filled porous pipe. Ansari and Deo [33] discussed the influence of magnetic field on two non-miscible type of viscous, incompressible, and electrically conducting fluid in a porous saturated rectangular channel. The impact of magnetic field on Stokesian flow of an incompressible micropolar fluid past a cylindrical tube enclosing an impermeable core coated by porous layer is studied by Deo et al. [34]. Maurya et al. [35] solved the Stokesian flow problem for an incompressible micropolar fluid within a porous saturated cylindrical channel and obtained the expressions for microrotation vectors, velocity vectors, and stream functions. Bhatti and Abdelsalam [36] studied the irreversibility process and entropy production in peristaltic flow of dusty magnetized Ree–Eyring fluid in a porous saturated channel with partial slip effects.

Nowadays, the area of thermal design and thermal exchange process encourages us to analyze the second law analysis, entropy generation minimization, and system design related concepts [37]. The second law analysis provides an essential and unique way for improving the appropriate design parameters in various thermofluid devices by minimizing the entropy generation because of fluid friction and thermal exchange. Carnot et al. [38] showed in his work that the dynamic development in heat transfer related areas is a consequence of entropy production analysis. They discussed various features of irreversibility arise due to the second law of thermodynamics. Bejan [39] introduced different sources of entropy production in various kinds of flows such as boundary layer flow, channel flow, flow in the entrance portion of the duct by using the concept of entropy generation

minimization (EGM). He defined discrete methodology and computing techniques for evaluating entropy production in the different heat transfer systems. Bejan [40] performed another study in which he addressed that the production of entropy in the convective thermal exchange process is mainly because of thermal production, thermal transportation and viscous nature of the fluid. Srinivas and his team [41–45] have done much work on the potential of entropy production and discussed the mechanism of entropy in different flow situations, flow conditions, and under different boundary conditions. Nezhad and Shahri [46] analyzed the impact of oriented magnetic field on thermal characteristics, flow profile, and entropy generation of non-miscible viscous fluids flowing inside an inclined duct and evaluated the thermal profile, flow velocity, and entropy production by adopting the homotopy analysis method. Mahmud and Fraser [47] presented numerical and analytical solutions of forced convective flow and entropy production of Newtonian viscous fluid through a porous material sandwiched by two parallel plates. He used Darcy–Brinkman model to formulate the governing equations of the problem. The influence of thermal radiation on thermal profile and entropy production of channel flows has a wide range of roles in solar technology, power plants, and nuclear reactors. Various approaches have been proposed by a number of researchers to analyze the entropy production due to thermal radiation in various participating media. Chauhan and Kumar [48] investigated the fully developed forced convective flow of fluid through a circular channel packed with highly porous medium. They used Darcy extended Brinkman–Forchheimer model for the modeling of fluid flow through porous medium. Gorla [49] studied the entropy production due to fully developed flow of non-Newtonian fluid in a vertical channel. Paoletti et al. [50] evaluated the exergetic losses due to different thermophysical flow parameters in a compact heat exchanger. Abbas et al. [51] studied the entropy production during the peristaltic blood-like transport of nanofluid in a two-dimensional channel with compliant walls. Bhatti et al. [52] investigated the impact of non-linear thermal radiation and magnetohydrodynamics (MHD) on entropy production analysis of an Eyring–Powell nanofluid over a permeable stretching surface. They used Chebyshev spectral collocation and Successive linearization method to the numerical solution of governing system of ordinary differential equations. Qing et al. [53] presented the influence of chemical reaction and thermal radiation on entropy production analysis of MHD Casson nanofluid through a porous stretching/shrinking surface. Riaz et al. [54] discussed the entropy production on peristaltic transport of non-Newtonian fluid in an asymmetric channel with boundary conditions. The emerging results of this study provide a benchmark for the study of entropy production with peristaltic pumping and mass transfer.

The models, as discussed above and which are originated from very well-known applications of fluid flow and heat transformation process, motivated us to consider and analyze the present problem. The subject of entropy analysis of immiscible fluids through porous regions is extensively studied in the above deliberated literature due to its growing need in modern technologies. The entropy analysis of immiscible fluids through a porous region is also an essential need to explore the working capacity of thermal technologies in terms of the conservation of energy. In the considered work, the main attention is given to the impact of thermal radiation and oriented magnetic field on the entropy generation of two non-miscible micropolar and Newtonian fluids in a porous saturated rectangular conduit. In this work, we did an analysis of thermal characteristics, entropy production, and flow profile of two non-miscible fluids in a channel which is filled with two different types of porous

materials. It is important to mention that the use of porous material in channels may help in reducing the noise when the non-miscible micropolar and Newtonian fluid takes place through it. Here, we focused on the consideration of two different types of porous materials through the study, one is for naturally occurring porous material and other is for man-made porous material. It is noticed that the upper limit of the porosity for the naturally occurring porous materials is 0.6 whereas the value of porosity for man-made porous substances is greater than 0.6 [25]. Some distinct man-made porous substances such as cement, air, filters, metallic foams, and so on take the value of porosity close to 1 [55]. In the present work, we also analyzed the impact of various emerging parameters such as porosity parameter, radiation parameter, Hartmann number, Reynolds number , and so on, on the entropy production characteristics, flow distribution, Bejan number, and thermal transformation of two non-miscible micropolar and Newtonian fluid flowing through the porous channel. Such study is very helpful in various scientific as well as engineering practical applications, e.g. making of cooling devices for various types of nuclear reactors. On the basis of past published work, no research work, which analyzed the significance of man-made and naturally occurring porous material on the entropy production characteristics of two non-miscible micropolar and Newtonian fluid in a duct, has been discussed yet. This fact encourages the authors to work in this direction for presenting some new results along with the validating results.

2. Governing fluid flow equations for non-miscible nature of Newtonian and micropolar fluids through a porous medium

The flow of Newtonian fluid in a rectangular porous enclosure with impact of oriented magnetic field as well as thermal radiation is addressed by energy balance equation, momentum equation, and mass balance equation.

The momentum equation which describes the flow velocity of Newtonian viscous fluid is given by Navier and Stokes [56]:

$$\rho\frac{\mathrm{D}\mathbf{v}}{\mathrm{D}t} = \mu\nabla^2\mathbf{v} - \nabla p + \mathbf{J}\times\mathbf{B} + \frac{2\mu}{3}\nabla(\nabla\cdot\mathbf{v}) - \frac{\mu}{K}\mathbf{v}. \tag{1}$$

In Equation (1), p, ρ, $\mathbf{v}$, and μ depict the applied pressure in flow domain, fluid density, velocity, and viscosity of Newtonian fluid respectively. The symbol K indicates the permeability of porous media. The electric current density $\mathbf{J}$ developed in the flow domain because of applied magnetic field $\mathbf{B}$. The magnetic body force is denoted by expression $\mathbf{J}\times\mathbf{B}$. In the present model, the flow field is subjected by a constant and oriented magnetic field which subtends an angle θ with the perpendicular direction of the flow domain.

Ohm's generalized law in a rectangular porous conduit takes the form:

$$\mathbf{J} = \sigma(\mathbf{E} + \mathbf{v}\times\mathbf{B}), \tag{2}$$

in which $\mathbf{E}$ and σ represent the electric field vector and electrical conductivity of electrically conducting immiscible fluid. The electric current density does not exist in the absence of an electric field and hence Equation (2) takes the form:

$$\mathbf{J} = \sigma(\mathbf{v}\times\mathbf{B}). \tag{3}$$

Thus the Lorentzian force $\mathbf{F} = \mathbf{J} \times \mathbf{B}$ develops in the flow field and the velocity vector acts in collinear and opposite direction. The Lorentzian force further transform and takes the form $\mathbf{F} = -\sigma B_0^2 \mathbf{v} \cos\theta$ where $\lambda = \cos\theta$ and $B_0 = |B|$ is the magnitude of applied magnetic field in the y-direction of the flow domain.

Darcy's generalized law [22] which describes the flow of fluid through porous media is presented as

$$\nabla p = -\frac{\mu}{K}\mathbf{v}. \tag{4}$$

In the current analysis, we employed the Brinkman model [23] for the flow analysis of Newtonian fluid in the porous regions. In Darcy's [22] equation, Brinkman [23] added viscous term $\mu_{eff}\nabla^2\mathbf{v}$ in which μ_{eff} depicts the effective viscosity of the fluid in porous material and it is different from the actual viscosity of fluid μ. Later on, Ochoa-Tapia and Whitaker [57] worked on Brinkman equation and evaluated that μ_{eff} is equivalent to $\frac{\mu}{\phi}$ by volume averaging technique, in which ϕ denotes the porosity property of Brinkman porous medium.

Hence, Brinkman equation for the flow of viscous fluid through porous medium with flow velocity $\mathbf{v}$, permeability K, and porosity ϕ takes the form as [7]

$$\nabla p = \frac{\mu}{\phi}\nabla^2\mathbf{v} - \frac{\mu}{K}\mathbf{v}. \tag{5}$$

Thus the equation of linear momentum which describes the flow velocity of Newtonian viscous fluid in porous media will become as [6,7]

$$\rho\frac{\mathrm{D}\mathbf{v}}{\mathrm{D}t} = \mathbf{J} \times \mathbf{B} - \nabla p + \frac{\mu}{\phi}\nabla^2\mathbf{v} - \frac{\mu}{K}\mathbf{v} + \frac{2\mu}{3}\nabla(\nabla \cdot \mathbf{v}). \tag{6}$$

Energy equation [14,58]:

$$\rho\frac{\mathrm{D}T}{\mathrm{D}t} = k\nabla^2 T - p(\nabla \cdot \mathbf{v}) + \mu\Gamma + \frac{\mathbf{J^2}}{\sigma} - \nabla \cdot q_r, \tag{7}$$

where

$$\Gamma = 2\left[\left(\frac{\partial w}{\partial z}\right)^2 + \left(\frac{\partial v}{\partial y}\right)^2 + \left(\frac{\partial u}{\partial x}\right)^2\right] + \left(\frac{\partial v}{\partial x} + \frac{\partial u}{\partial y}\right)^2 + \left(\frac{\partial u}{\partial z} + \frac{\partial w}{\partial x}\right)^2 + \left(\frac{\partial w}{\partial y} + \frac{\partial v}{\partial z}\right)^2.$$

Equation of continuity [56]:

$$\frac{\partial \rho}{\partial t} + \nabla \cdot (\rho\mathbf{v}) = 0. \tag{8}$$

In the above equation, temperature profile and thermal conductivity of Newtonian viscous fluid are depicted by term T, k respectively. The dissipation function of the energy equation for Newtonian viscous fluid is expressed by the symbol Γ. The radiative thermal flux for Newtonian viscous fluid is represented by the last term of Equation (7).

The radiative thermal exchange can be approximated by using the concept of Rosseland's diffusion approximation and hence the radiative heat flux term can be derived as [41]

$$q_r = -\frac{4}{3}\frac{\sigma^*}{k^*}\frac{\mathrm{d}T^4}{\mathrm{d}y}. \tag{9}$$

Here σ^* and k^* are the Stefan–Boltzmann constant and Rosseland's mean absorption coefficient respectively. It is considered that temperature differences in the flow domain are too

small and hence we express the term T^4 in a linear combination of temperature. For this, we adopt the Taylor series expansion about T_0. The above assumptions lead to the following expression:

$$T^4 = \sum_{n=0}^{\infty} \frac{1}{n!}[(T^4)^{(n)}]_{T=T_0}(T - T_0)^n.$$

or

$$T^4 = {T_0}^4 + ((T^4)')|_{T=T_0}(T - T_0) + \frac{1}{2!}((T^4)'')|_{T=T_0}(T - T_0)^2 + - - -$$

$$T^4 = {T_0}^4 + 4{T_0}^3(T - T_0) + 6{T_0}^2(T - T_0)^2 + - - - \tag{10}$$

and removing the higher-order terms except for first degree term, we get

$$T^4 = 4{T_0}^3 T - 3{T_0}^4. \tag{11}$$

Differentiating Equation (9) and using Equation (11), we have

$$\frac{\mathrm{d}q_r}{\mathrm{d}y} = -\frac{16\sigma^* {T_0}^3}{3k^*}\frac{\mathrm{d}^2 T}{\mathrm{d}y^2}. \tag{12}$$

The flow of micropolar fluid inside a rectangular porous conduit under the impact of an oriented magnetic field as well as thermal radiation is given by the energy balance equation, momentum balance equation together with mass balance equation. The constitutive equations of micropolar fluid are given by Eringen [1,2].

Thus the equation of linear momentum which describes the flow velocity of micropolar fluid in porous media will become as [6,10]

$$\rho\frac{\mathrm{D}\mathbf{v}}{\mathrm{D}t} = -\nabla p + \frac{\kappa}{\phi}\nabla \times \omega - \frac{(\mu + \kappa)}{\phi}\nabla \times \nabla \times \mathbf{v} + (\xi_1 + 2\mu + \kappa)\nabla(\nabla \cdot \mathbf{v})$$
$$+ \mathbf{J} \times \mathbf{B} - \frac{\mu + \kappa}{K}\mathbf{v} + \rho\mathbf{g}. \tag{13}$$

Here (ξ_1, μ, κ) are designated for viscosity coefficients or material constants of micropolar fluid, in which κ and μ denote the Eringen vortex viscosity and Newtonian dynamic viscosity respectively. The terms ω, $\mathbf{v}$ denote the angular and linear velocity vectors respectively.

Equation of angular momentum [6,10]:

$$\rho j\frac{\mathrm{D}\omega}{\mathrm{D}t} = \rho\mathbf{l} - 2\kappa\omega + \kappa\nabla \times \mathbf{v} - \gamma\nabla \times \nabla \times \omega + (\alpha_1 + \beta + \gamma)\nabla(\nabla \cdot \omega). \tag{14}$$

Here $(\alpha_1, \beta, \gamma)$ are symbolized for angular viscosities, $\mathbf{l}$ depicts the body couple defined per unit mass and symbol j denotes the gyration coefficient. The following inequalities hold for the above-discussed parameters [44].

$| \beta | \leq \gamma; \kappa \geq 0; 3\alpha_1 + \gamma + \beta \geq 0; \kappa + 2\mu \geq 0; 3\xi + \kappa + 2\mu \geq 0; \gamma \geq 0.$

Energy equation [10,44]:

$$\rho\frac{\mathrm{D}T}{\mathrm{D}t} = -p(\nabla \cdot \mathbf{v}) + \rho\Sigma - (\nabla \cdot \mathbf{h}) + \frac{\mathbf{J}^2}{\sigma} + \frac{\mu + \kappa}{K}\mathbf{v}^2 - \nabla \cdot q_r, \tag{15}$$

where the expression for $\rho\Sigma$ takes the value:

$$\rho\Sigma = \xi_1(\nabla\cdot\mathbf{v})^2 + \gamma(\nabla\omega:\nabla\omega) + 4\frac{\kappa}{\phi}\left(\frac{1}{2}\nabla\times\mathbf{v}-\omega\right)^2 + \alpha_1(\nabla\cdot\omega)^2 + 2\frac{\mu}{\phi}(D:D) + \beta(\nabla\omega:(\nabla\omega)^T).$$

In the theory of microfluids, the deformation rate tensor is denoted by D, which takes the form $\frac{1}{2}(\mathbf{v}_{i,j}+\mathbf{v}_{j,i})$. In energy equation, mechanical energy per unit mass is expressed by term Σ. The coefficients κ, α_1, β and γ are designated in such a way that if $\kappa=\alpha_1=\beta=\gamma=0$ as well as $\mathbf{I}$ vanishes in Equation (14) then $\omega=0$ and system of equations transformed into the classical hydrodynamical Navier–Stokes equations. The symbol h is designated for thermal flux of micropolar fluid which takes the form $-k\nabla T$, here k stands for heat conductivity.

Continuity equation [42,44]:

$$\frac{\partial\rho}{\partial t}+\nabla\cdot(\rho\mathbf{v})=0. \tag{16}$$

3. Statement and solution of the considered problem

3.1. Mathematical formulation

In this study, the two-layered non-miscible flow of micropolar and Newtonian fluid system through a rectangular porous conduit with oriented magnetic field and thermal radiation effect has been discussed. In this model, the Newtonian fluid layer and micropolar liquid layer lie in the bottom and upper porous regions of the conduit respectively. The geometrical configuration and coordinate system are displayed in Figure 1. The model is confined by two isothermal parallel walls expanding in x- and y -directions. It is considered that the height of the conduit is too much small as compared to its length and the flow of non-miscible fluid takes place because of the applied pressure gradient which is functioned along axial direction of the flow system. The rectangular conduit is designated in such a way that the top and bottom walls are of 2 h distance apart and the walls are kept at static position. Due to immiscibility, the Newtonian and micropolar fluids cannot mixed up with each other. An oriented magnetic field acts on the flow domain and it subtends an angle $\theta, (0<\theta<\pi/2)$ with y-axis of the flow field. In this flow problem, the top $(0\le y\le h)$ and bottom zones $(-h\le y\le 0)$ of the flow conduit are saturated by porous material having different nature of porosity ϕ_1 and ϕ_2 respectively. The permeability of upper and bottom porous zones of the flow conduit is taken as K_1 and K_2 respectively. According to these circumstances, the micropolar liquid layers confined in upper porous domain $(0\le y\le h)$ with flow properties such as viscosity μ_1, porosity ϕ_1, flow velocity u_1, permeability K_1, electrical conductivity σ_1, and thermal properties such as thermal conductivity k_1 and thermal characteristics T_1. The Newtonian liquid layers confined in bottom porous domain $(-h\le y\le 0)$ with flow properties such as viscosity μ_2, porosity ϕ_2, flow velocity u_2, electrical conductivity σ_2, permeability K_2, and thermal properties such as thermal conductivity k_2, thermal characteristics T_2.

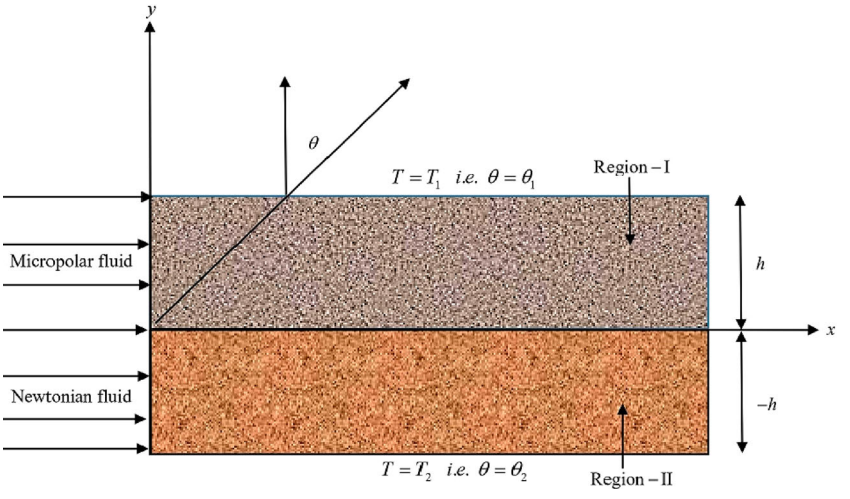

Figure 1. Mathematical model.

3.2. Problem description and governing equations

According to the physical flow situations of the problem, authors adopted following assumptions for formulating the governing equations of thermal field and flow distribution of non-miscible fluid inside a rectangular porous conduit. These assumptions are compatible throughout the problem.

- The two non-miscible fluid layers of micropolar and Newtonian fluid are governed by fully developed, axisymmetric, unidirectional, steady, and laminar flow regimes.
- The transport characteristics of two-phase micropolar and Newtonian fluid are supposed to be constant.
- The porous media in rectangular conduit is homogeneous.

With the above assumptions, the governing field equations (13)–(16) for an incompressible, radiative, magnetized, and steady flow regime of micropolar fluid within a static rectangular porous conduit are addressed by the equation of continuity, momentum, and energy respectively.

Continuity equation [42,44]:

$$\nabla \cdot \mathbf{v}_1 = 0. \tag{17}$$

Equation of linear momentum [6,10]:

$$\frac{(\mu_1 + \kappa)}{\phi_1}\nabla^2 \mathbf{v}_1 + \frac{\kappa}{\phi_1}\nabla \times \omega - \nabla p + \mathbf{J} \times \mathbf{B} - \frac{\mu_1 + \kappa}{K_1}\mathbf{v}_1 = 0. \tag{18}$$

Equation of angular momentum [6,10]:

$$\gamma \nabla^2 \omega - \kappa(2\omega - \nabla \times \mathbf{v}_1) = 0. \tag{19}$$

Energy equation [10,44]:

$$k_1\nabla^2 T_1 + 2\frac{\mu_1}{\phi_1}(D:D) + 4\frac{\kappa}{\phi_1}\left(\frac{1}{2}\nabla\times\mathbf{v}_1 - \omega\right)^2 + \beta(\nabla\omega:(\nabla\omega)^T) + \frac{J^2}{\sigma} + \frac{\mu_1+\kappa}{K_1}\mathbf{v}_1^2 - \nabla\cdot q_r = 0. \tag{20}$$

The governing field equations (6)–(8) for an incompressible, radiative, magnetized, and steady flow regime of Newtonian fluid within a static rectangular porous conduit are addressed by continuity, Brinkman momentum, and energy equation respectively.

Continuity equation [56]:

$$\nabla\cdot\mathbf{v}_2 = 0. \tag{21}$$

Equation of linear momentum [6,59]:

$$\frac{\mu_2}{\phi_2}\nabla^2\mathbf{v}_2 - \nabla p + \mathbf{J}\times\mathbf{B} - \frac{\mu_2}{K_2}\mathbf{v}_2 = 0. \tag{22}$$

Energy equation [14,58]:

$$k_2\nabla^2 T_2 + \frac{\mu_2}{\phi_2}\Gamma + \frac{J^2}{\sigma} + \frac{\mu_2}{K_2}\mathbf{v}_2^2 - \nabla\cdot q_r = 0. \tag{23}$$

Since, due to the consideration of mass balance equation for an incompressible micropolar fluid in a fully developed flow regime, the axial velocity component of micropolar fluid will be a function of y only whereas its y-directional velocity component will vanish. Thus, under the above-mentioned assumptions of the problem, the component form of microrotational and linear flow velocity vector of micropolar fluid in upper porous region of the conduit can be expressed as $\omega = (0,0,\omega)$ and $\mathbf{v_1} = (u_1,0,0)$ respectively, where $u_1 = u_1(y)$.

After applying the above assumptions with thermal radiation and oriented magnetic field effect, the governing coupled differential equation for angular velocity, temperature profile, and linear flow velocity of the micropolar fluid will become as follows:

Conservation of linear momentum [6,7]:

$$\frac{(\mu_1+\kappa)}{\phi_1}\frac{\mathrm{d}^2u_1}{\mathrm{d}y^2} + \frac{\kappa}{\phi_1}\frac{\mathrm{d}\omega}{\mathrm{d}y} - \sigma_1 B_0^2\lambda^2 u_1 - \frac{\mu_1+\kappa}{K_1}u_1 = \frac{\mathrm{d}p}{\mathrm{d}x}. \tag{24}$$

Conservation of angular momentum [6,7]:

$$\gamma\frac{\mathrm{d}^2\omega}{\mathrm{d}y^2} - \kappa\left(2\omega + \frac{\mathrm{d}u_1}{\mathrm{d}y}\right) = 0. \tag{25}$$

Ahmadi [60] introduced the value of symbol γ which is expressed as

$$\gamma = \left(\mu_1 + \frac{\kappa}{2}\right)i. \tag{26}$$

The symbol i designated for microinertia density.

Energy equation [42,44]:

$$k_1\frac{\mathrm{d}^2T_1}{\mathrm{d}y^2}+\frac{\mu_1}{\phi_1}\left(\frac{\mathrm{d}u_1}{\mathrm{d}y}\right)^2+\frac{\kappa}{\phi_1}\left(\frac{\mathrm{d}u_1}{\mathrm{d}y}+2\omega\right)^2+\beta\left(\frac{\mathrm{d}\omega}{\mathrm{d}y}\right)^2 + \sigma_1 B_0^2\lambda^2{u_1}^2+\frac{\mu_1+\kappa}{K_1}{u_1}^2-\frac{\mathrm{d}q_{r_1}}{\mathrm{d}y}=0. \tag{27}$$

Since, due to the consideration of mass balance equation for an incompressible Newtonian fluid in a fully developed flow regime, the axial velocity component of Newtonian fluid will be a function of y only whereas its y-directional velocity component will vanish. Thus under the above-mentioned assumptions of the problem, the component form of linear flow velocity vector of Newtonian fluid in bottom porous region of the conduit can be expressed as $\mathbf{v_2}=(u_2,0,0)$ respectively, where $u_2=u_2(y)$.

After applying the above assumptions with thermal radiation and oriented magnetic field effect, the governing coupled differential equation for angular velocity, temperature profile, and linear flow velocity of the Newtonian fluid will become as follows:

Conservation of linear momentum [6,7]:

$$\frac{\mu_2}{\phi_2}\frac{\mathrm{d}^2u_2}{\mathrm{d}y^2}-\frac{\mu_2}{K_2}u_2-\sigma_2B_0^2\lambda^2u_2=\frac{\mathrm{d}p}{\mathrm{d}x}. \tag{28}$$

Conservation of energy [14,58]:

$$k_2\frac{\mathrm{d}^2T_2}{\mathrm{d}y^2}+\frac{\mu_2}{\phi_2}\left(\frac{\mathrm{d}u_2}{\mathrm{d}y}\right)^2+\frac{\mu_2}{K_2}{u_2}^2+\sigma_2B_0^2\lambda^2{u_2}^2-\frac{\mathrm{d}q_{r_2}}{\mathrm{d}y}=0. \tag{29}$$

3.3. Solution methodology

To transform the converted governing system of ordinary differential equations into normalized form, the following dimensionless variables are deployed:

$$u_i^*=\frac{u_i}{U_0},\ i=1,2,\quad y^*=\frac{y}{h},\quad x^*=\frac{x}{h},\quad p^*=\frac{p}{\rho_1U_0^2},$$
$$\omega^*=\frac{\omega h}{U_0},\quad n_\mu=\frac{\mu_2}{\mu_1},\quad n_k=\frac{k_2}{k_1},\quad Da^2=\frac{h^2}{K_1}$$
$$n_\sigma=\frac{\sigma_2}{\sigma_1},\quad \alpha=\frac{\kappa}{\mu_1},\quad \theta_i=\frac{T_i^*-T_0}{\Delta T},\quad Br=\frac{\mu_1U_0^2}{k_1\Delta T},$$
$$\delta=\frac{\beta}{\mu_1h^2},\quad Ha=B_0h\sqrt{\frac{\sigma_1}{\mu_1}},\quad Re=\frac{\rho_1U_0h}{\mu_1}$$
$$L^2=\frac{\gamma}{\mu_1h^2\alpha},\quad n_K=\frac{K_2}{K_1},\quad Nr=\frac{4\sigma^*{T_0}^3}{k^*k_1}.$$

The non-dimensional numbers such as Reynolds number, permeability parameter, Hartmann number, and Brinkman number are expressed by the symbol *Re*, *Da*, *Ha*, and *Br* respectively. The dimensionless variables such as n_σ, n_k, n_K, and n_μ represent the electrical conductivity ratio, thermal conductivity ratio, permeability ratio of porous medium, and viscosity ratio of two-phase flow system respectively. The quantities ΔT denote the

characteristics temperature which is expressed as $\Delta T = T_1^* - T_2^*$, in which $T_1^* > T_2^*$. The characteristic flow velocity is depicted by the symbol U_0. The scaling parameter is denoted by symbol L.

With the consideration of these dimensionless variables in Equations (24)–(29) and removing the $*$ symbol, we addressed the following simplified form of governing differential equations:

Region-1 ($-h \le y \le 0$):

$$\frac{\mathrm{d}^2 u_1}{\mathrm{d}y^2} + \frac{\alpha}{1+\alpha}\frac{\mathrm{d}\omega}{\mathrm{d}y} - \frac{(Ha^2\lambda^2 + Da^2(1+\alpha))}{1+\alpha}\phi_1 u_1 - \frac{ReP}{1+\alpha}\phi_1 = 0, \tag{30}$$

$$\frac{\mathrm{d}^2\omega}{\mathrm{d}y^2} - \frac{1}{L^2}\left(2\omega + \frac{\mathrm{d}u_1}{\mathrm{d}y}\right) = 0, \tag{31}$$

$$\left(1+\frac{4}{3}Nr\right)\frac{\mathrm{d}^2\theta_1}{\mathrm{d}y^2} + \frac{Br}{\phi_1}\left[\left(\frac{\mathrm{d}u_1}{\mathrm{d}y}\right)^2 + \alpha\left(\frac{\mathrm{d}u_1}{\mathrm{d}y} + 2\omega\right)^2 + \delta\phi_1\left(\frac{\mathrm{d}\omega}{\mathrm{d}y}\right)^2 + (Ha^2\lambda^2 + (1+\alpha)Da^2)\phi_1 u_1^2\right] = 0, \tag{32}$$

where $P = \frac{\mathrm{d}p}{\mathrm{d}x}$.

Region-2 ($0 \le y \le h$):

$$\frac{\mathrm{d}^2 u_2}{\mathrm{d}y^2} - \left(\frac{Da^2}{n_K} + \frac{n_\sigma}{n_\mu}Ha^2\lambda^2\right)\phi_2 u_2 - \frac{ReP\phi_2}{n_\mu} = 0, \tag{33}$$

$$\left(1+\frac{4}{3}\frac{Nr}{n_k}\right)\frac{\mathrm{d}^2\theta_2}{\mathrm{d}y^2} + \frac{Brn_\mu}{n_k\phi_2}\left[\left(\frac{\mathrm{d}u_2}{\mathrm{d}y}\right)^2 + \left(\frac{Da^2}{n_K} + \frac{n_\sigma}{n_\mu}Ha^2\lambda^2\right)\phi_2 u_2^2\right] = 0. \tag{34}$$

We employed reliable technique for evaluating the closed form solution of Equations (30)–(34). Thus the flow variable of incompressible micropolar fluid in the top porous region and incompressible Newtonian fluid in the bottom porous region of the flow conduit is as follows.

The flow velocity distribution for micropolar fluid is

$$u_1(y) = c_1\,\mathrm{e}^{-\epsilon y} + c_2\,\mathrm{e}^{\epsilon y} + c_3\,\mathrm{e}^{-\tau y} + c_4\,\mathrm{e}^{\tau y} + \frac{PRe\phi_1}{Da^2\phi_1 + Da^2\alpha\phi_1 + Ha^2\lambda^2\phi_1}. \tag{35}$$

The angular velocity distribution for micropolar fluid is

$$w(y) = \eta(-c_1\,\mathrm{e}^{-\epsilon y} + c_2\,\mathrm{e}^{\epsilon y}) + \xi(-c_3\,\mathrm{e}^{-\tau y} + c_4\,\mathrm{e}^{\tau y}). \tag{36}$$

The temperature characteristics for micropolar fluid is

$$\begin{aligned}\theta_1(y) = {} & Br_1(-8\epsilon_1{}^2 c_1 PRe\xi\phi_1\,\mathrm{e}^{-y\epsilon} - 8\epsilon_1{}^2 c_2 PRe\xi\phi_1\,\mathrm{e}^{y\epsilon} \\ & - 8\tau_1{}^2 c_1 PRe\xi\phi_1\,\mathrm{e}^{-y\tau} - 8\tau_1{}^2 c_2 PRe\xi\phi_1\,\mathrm{e}^{y\tau}) \\ & + Br_1(\mathrm{e}^{2y\epsilon}\epsilon_1{}^2\xi c_2{}^2((1+\alpha)\epsilon^2 + 4\alpha\epsilon\eta + 4\alpha\eta^2 + \chi) \\ & + \mathrm{e}^{2y\tau}\tau_1{}^2\xi c_4{}^2((1+\alpha)\tau^2 + 4\alpha\tau\zeta + 4\alpha\zeta^2 + \Psi))\end{aligned}$$

$$
\begin{aligned}
&+ Br_1(8\,e^{(\epsilon-\tau)y}(\epsilon-\tau)_1{}^2\xi c_2c_3(-\Phi+\varphi) + 8\,e^{(-\epsilon+\tau)y}(\epsilon-\tau)_1{}^2\xi c_1c_4(-\Phi+\varphi))\\
&+ Br_1(8\,e^{-(\epsilon+\tau)y}(\epsilon+\tau)_1{}^2\xi c_1c_3(\Phi+\varphi) + 8\,e^{(\epsilon+\tau)y}(\epsilon+\tau)_1{}^2\xi c_2c_4(\Phi+\varphi))\\
&+ 2Br_1y^2(-2\xi((1+\alpha)\epsilon^2c_1c_2 + 4\alpha\epsilon\eta c_1c_2 + \tau^2c_3c_4)\\
&- 2\xi(\alpha(4\eta^2c_1c_2 + (2\zeta+\tau)^2c_3c_4))\\
&+ 2Br_1(P^2Re^2 + 2\xi(\xi\phi_1(c_1c_2 + c_3c_4))) + 2Br_1(2\xi(\delta(\epsilon^2\eta^2c_1c_2 + \zeta^2\tau^2c_3c_4)))\phi_1\\
&+ Br_1(\,e^{-2y\epsilon}\xi\epsilon_1{}^2\tau_1\tau c_1{}^2((1+\alpha)\epsilon^2 + 4\alpha\epsilon\eta + 4\alpha\eta^2 + \chi))\\
&+ Br_1(e^{-2y\tau}\xi\tau_1{}^2\epsilon_1\epsilon c_3{}^2((1+\alpha)\tau^2 + 4\alpha\tau\zeta + 4\alpha\zeta^2 + \Psi)) + c_5 + yc_6. \qquad (37)
\end{aligned}
$$

The flow velocity distribution for Newtonian fluid is

$$
u_2(y) = c_7\,e^{-y\Lambda} + c_8\,e^{y\Lambda} - \frac{n_KReP}{Da^2n_\mu + Ha^2\lambda^2n_Kn_\sigma} \qquad (38)
$$

The temperature characteristics for Newtonian fluid is

$$
\begin{aligned}
\theta_2(y) = &-Br_2(e^{2y\Lambda}c_8{}^2\sqrt{n_K}n_\mu(Da^2n_\mu + Ha^2\lambda^2n_Kn_\sigma)) - Br_2(P^2Re^2y^2{n_K}^{3/2}\phi_2) + c_9\\
&+ yc_{10}Br_2(4\,e^{-\Lambda y}PRec_7{n_K}^{3/2}n_\mu + 4\,e^{\Lambda y}PRec_8{n_K}^{3/2}n_\mu)\\
&- Br_2(\,e^{-2y\Lambda}c_7{}^2\sqrt{n_K}n_\mu(Da^2n_\mu + Ha^2\lambda^2n_Kn_\sigma)), \qquad (39)
\end{aligned}
$$

where

$$
\epsilon = \sqrt{A_1 - \sqrt{{A_1}^2 - 4A_2}}, \qquad (40)
$$

$$
\tau = \sqrt{A_1 + \sqrt{{A_1}^2 - 4A_2}}, \qquad (41)
$$

$$
A_1 = \frac{1}{L^2(1+\alpha)} + \frac{\alpha}{2L^2(1+\alpha)} + \frac{Da^2\phi_1}{2(1+\alpha)} + \frac{Da^2\alpha\phi_1}{2(1+\alpha)} + \frac{Ha^2\lambda^2\phi_1}{2(1+\alpha)} \qquad (42)
$$

$$
A_2 = \frac{Da^2\phi_1}{2L^2(1+\alpha)} + \frac{Da^2\alpha\phi_1}{2L^2(1+\alpha)} + \frac{Ha^2\lambda^2\phi_1}{2L^2(1+\alpha)} \qquad (43)
$$

$$
\eta = \left(\frac{L^2\xi\phi_1}{2\alpha} - \frac{1}{2} - \frac{L^2(1+\alpha)\epsilon^2}{2\alpha}\right)\epsilon, \qquad (44)
$$

$$
\zeta = \left(\frac{L^2\xi\phi_1}{2\alpha} - \frac{1}{2} - \frac{L^2(1+\alpha)\tau^2}{2\alpha}\right)\tau, \qquad (45)
$$

$$
\xi = (Ha^2\lambda^2 + Da^2(1+\alpha)), \qquad (46)
$$

$$
\varphi = (Ha^2\lambda^2 + Da^2(1+\alpha) + \delta\epsilon\zeta\eta\tau)\phi_1, \qquad (47)
$$

$$
\chi = (Ha^2\lambda^2 + Da^2(1+\alpha) + \delta\epsilon^2\eta^2)\phi_1, \qquad (48)
$$

$$
\Psi = (Ha^2\lambda^2 + Da^2(1+\alpha) + \delta\tau^2\zeta^2)\phi_1, \qquad (49)
$$

$$
\Phi = \epsilon\tau + \alpha(\epsilon+2\eta)(2\zeta+\tau), \qquad (50)
$$

$$
\Lambda = \frac{\sqrt{Da^2n_\mu + Ha^2\lambda^2n_Kn_\sigma}\sqrt{\phi_2}}{\sqrt{n_K}\sqrt{n_\mu}}, \qquad (51)
$$

$$Br_1 = \frac{3Br}{4(3+4Nr)\xi}, \quad \epsilon_1 = \frac{1}{\epsilon}, \quad \tau_1 = \frac{1}{\tau}, \quad (\epsilon+\tau)_1 = \frac{1}{(\epsilon+\tau)}, \quad (\epsilon-\tau)_1 = \frac{1}{(\epsilon-\tau)}, \tag{52}$$

$$Br_2 = \frac{3Br}{2(4Nr+3n_k)\sqrt{n_k}(Da^2 n_\mu + Ha^2\lambda^2 n_K n_\sigma)\phi_2}. \tag{53}$$

General solutions of the governing system of equations are obtained by evaluating the values of arbitrary constants $c_1, c_2, c_3, c_4, c_5, c_6, c_7, c_8, c_9, c_{10}$, which are involved in the above equations. These constants are determined by the appropriate boundary conditions which are discussed in the next section.

3.4. Boundary conditions

The fluid–fluid interface possesses numerous varieties of conditions in various flow channels. From a mechanical viewpoint, the continuity of shear stress, velocity component, convective heat transfer, and thermal flux occurs at the porous–porous interface. The bottom and top static isothermal plates of the conduit are expressed by $y = -1$ and $y = 1$ respectively while the porous–porous interface is denoted by $y = 0$.

The shear stress and flow velocity component across $y = 0$ are continuous [6].

$$\frac{(1+\alpha)}{\phi_1}\frac{du_1}{dy} + \frac{\alpha}{\phi_1}\omega = \frac{n_\mu}{\phi_2}\frac{du_2}{dy}. \tag{54}$$

$$u_1(y) = u_2(y), \tag{55}$$

At the porous–porous interface, the convective heat transfer and thermal flux are continuous.

$$\theta_1(y) = \theta_2(y), \tag{56}$$

$$\frac{d\theta_1}{dy} = n_k\frac{d\theta_2}{dy}. \tag{57}$$

The constant angular velocity across the porous–porous interface of the conduit is given by Ariman et al. [4].

$$\frac{d\omega}{dy} = 0 \text{ at } y = 0. \tag{58}$$

The convective thermal exchange at the upper and bottom isothermal wall of the conduit is given by

$$\theta_1 = 1, \text{ at } y = 1, \tag{59}$$

$$\theta_2 = 0, \text{ at } y = -1. \tag{60}$$

It is well known that the micro-rotation vector at the porous wall surface = angular velocity of micropolar fluid particles at the porous boundary. This condition is known as hyper-stick condition which takes the form:

$$\omega_{wall} = n(\nabla \times \mathbf{v_1}), \text{ in which } 0 \le n \le 1. \tag{61}$$

In Equation (61), n determines the concentration or interaction of the micropolar fluid particles with the porous boundaries of the conduit. The value of ω becomes zero when we put

the value of n equal to zero, this shows that for $n = 0$, the rotational motion of micro-fluid particle becomes zero at porous boundaries of the duct [11]. This may happen because of the strong concentration of micro-fluid particles.

Here, the angular velocity is zero at the upper wall surface which is also known as no-spin condition [12].

$$\omega(y) = 0 \text{ at } y = 1. \tag{62}$$

In the prescribed model, no-slip conditions were essentially imposed on upper and bottom wall surfaces of the duct [42].

$$u_1(y) = 0 \text{ at } y = 1, \tag{63}$$

$$u_2(y) = 0 \text{ at } y = -1. \tag{64}$$

4. Entropy production number and Bejan number

4.1. Production of entropy in a rectangular porous enclosure

The production of entropy is a thermodynamic property that analyzes the destruction of useful energy in any thermal and engineering procedure which involves in fluid flow, thermal exchange, and mass transfer phenomenon. The analysis of entropy production is determined by thermal exchange and velocity distribution. In the current problem, the production of entropy arises because of fluid friction, applied electromagnetic field, porous media, and thermal radiation.

The production of entropy per unit volume for radiative, incompressible, magnetized, electrically conducting, and viscous micropolar fluid flow within the porous medium takes the form [41,44] :

$$(S_1)_G = \frac{k_1}{T_0^2}\left[1 + \frac{16\sigma^* T_0^3}{3k^* k_1}\right]\left(\frac{\partial T_1}{\partial y}\right)^2 + \frac{\beta_1}{T_0}\left(\frac{\partial \omega}{\partial y}\right)^2 + \frac{\mu_1}{T_0\phi_1}\left(\frac{\partial u_1}{\partial y}\right)^2 + \frac{k_1}{T_0\phi_1}\left(\frac{\partial u_1}{\partial y} + 2\omega\right)^2 + \frac{\mu_1 + \kappa}{K_1 T_0}{u_1}^2 + \frac{\sigma_1 B_0^2 \lambda^2 u_1^2}{T_0}. \tag{65}$$

In Equation (65), first, fifth, and sixth terms respectively represent the production of entropy in micropolar fluid because of radiative heat transfer, presence of porous media and action of the oriented magnetic field. The remaining term depicts the entropy production because of fluid friction through the porous conduit.

The analysis of volumetric entropy production rate for radiative, incompressible, magnetized, electrically conducting and viscous Newtonian fluid flow within the porous conduit takes the form [48]:

$$(S_2)_G = \frac{k_2}{T_0^2}\left[1 + \frac{16\sigma^* T_0^3}{3k^* k_2}\right]\left(\frac{\partial T_2}{\partial y}\right)^2 + \frac{\mu_2}{T_0\phi_2}\left(\frac{\partial u_2}{\partial y}\right)^2 + \frac{\mu_2}{K_2 T_0}{u_2}^2 + \frac{\sigma_2 B_0^2 \lambda^2 u_2^2}{T_0}. \tag{66}$$

In Equation (66), first, third, and fourth terms respectively represent the production of entropy in Newtonian fluid because of radiative heat transfer, presence of porous media, and action of an oriented magnetic field. The second term depicts the entropy production because of fluid friction through the porous conduit.

It has been introduced by Bejan [24,39] that characteristics entropy production rate is determined by

$$S_{G,C} = \left[\frac{k_1(\Delta T)^2}{h^2 T_0^2}\right]. \tag{67}$$

In Equation (67) $\Delta T, T_0$, and h respectively, described the difference in temperature profile between the fixed wall surface of the duct, reference temperature, and half distance between the wall of the conduit.

The entropy production number is a dimensionless quantity which is the fraction of volumetric entropy production rate $(S_i)_G, i = 1, 2$ to the characteristics entropy production rate $S_{G,C}$

The production of entropy for radiative, incompressible, magnetized, and electrically conducting micropolar fluid flow inside a porous conduit takes the form:

$$Ns_1 = \left[1 + \frac{4}{3}Nr\right]\left(\frac{d\theta_1}{dy}\right)^2 + \frac{Br}{\phi_1}\left[\left(\frac{du_1}{dy}\right)^2 + \alpha\left(\frac{du_1}{dy} + 2\omega\right)^2 + \delta\phi_1\left(\frac{d\omega}{dy}\right)^2 + (Ha^2\lambda^2 + (1+\alpha)Da^2)\phi_1 u_1^2\right] \tag{68}$$

The production of entropy for radiative, incompressible, magnetized, and electrically conducting Newtonian fluid flow inside a porous conduit takes the form:

$$Ns_2 = \left[1 + \frac{4}{3}\frac{Nr}{n_k}\right]\left(\frac{d\theta_2}{dy}\right)^2 + \frac{Brn_\mu}{n_k\phi_2}\left[\left(\frac{du_2}{dy}\right)^2 + \left(\frac{Da^2}{n_k} + \frac{n_\sigma}{n_\mu}Ha^2\lambda^2\right)\phi_2 u_2^2\right] \tag{69}$$

$$Ns_i = Ny_i + Nf_i. \tag{70}$$

In Equation (70), Ny_i depicts the production of entropy because of radiative heat transfer and Nf_i represents the production of entropy arises because of fluid friction, magnetic field, and porous media.

4.2. Bejan number distribution

The irreversibility distribution ratio is the fraction of entropy production because of fluid friction (Nf_i) to the entropy production because of radiative thermal exchange (Ny_i), i.e.

$$p_i = \frac{Nf_i}{Ny_i}, \quad i = 1, 2. \tag{71}$$

The nature of irreversibility distribution is classified according to the different ranges of p_i. The radiative heat transfer irreversibility, fluid friction irreversibility, and irreversibility distribution due to combining effect of radiative thermal transportation and fluid friction is classified in the ranges of $0 < p_i < 1, p_i > 1$, and $p_i = 1$ respectively [42].

Bejan number is an important thermodynamic parameter in advanced thermal engineering. It is an alternative parameter of irreversibility distribution mechanism which is introduced by Paoletti et al. [50] in their work. Bejan number distribution is obtained,

with the division of the entropy generation because of radiative heat transfer by the total entropy production arises within the flow system.

$$Be_i = \frac{Ny_i}{Ns_i} = \frac{Ny_i}{Ny_i + Nf_i} = \frac{1}{1+p_i}, \quad i = 1, 2. \tag{72}$$

The Bejan number distribution is classified in three different ranges. From Equation (72), $Be = 0$ depicts that irreversibility generated by radiative heat transfer is zero, $Be = 1$ denotes that the irreversibility generated by fluid friction, magnetic field, and porous is negligible; $Be = 0.5$ shows that irreversibility generated by radiative heat transfer and other factors such as fluid friction, magnetic field, and porous media (all) are same.

Thus the Bejan number profile for the flow regime of micropolar fluid through a static rectangular porous enclosure under the influence of oriented magnetic field and thermal radiation is given as [41,44]

$$Be_1 = \frac{\left[1+\frac{4}{3}Nr\right]\left(\frac{d\theta_1}{dy}\right)^2}{\left[1+\frac{4}{3}Nr\right]\left(\frac{d\theta_1}{dy}\right)^2 + \frac{Br}{\phi_1}\left[\left(\frac{du_1}{dy}\right)^2 + \alpha\left(\frac{du_1}{dy}+2\omega\right)^2 + \delta\phi_1\left(\frac{d\omega}{dy}\right)^2 + (Ha^2\lambda^2 + (1+\alpha)Da^2)\phi_1 u_1^2\right]}. \tag{73}$$

The Bejan number profile for the flow regime of Newtonian fluid through a static rectangular porous enclosure under the influence of oriented magnetic field and thermal radiation is given as [46]

$$Be_2 = \frac{\left[1+\frac{4}{3}\frac{Nr}{n_k}\right]\left(\frac{d\theta_2}{dy}\right)^2}{\left[1+\frac{4}{3}\frac{Nr}{n_k}\right]\left(\frac{d\theta_2}{dy}\right)^2 + \frac{Brn_\mu}{n_k\phi_2}\left[\left(\frac{du_2}{dy}\right)^2 + \left(\frac{Da^2}{n_K} + \frac{n_\alpha}{n_\mu}Ha^2\lambda^2\right)\phi_2 u_2^2\right]}. \tag{74}$$

5. Analysis of the results

A growing body of literature has examined the thermal characteristics and flow field of non-miscible fluid through various geometrical configuration and flow situation because of its dynamic applications in various emerging fields of science. Our study provides additional support for entropy generation analysis of the two-layered non-miscible flow of micropolar and Newtonian fluid through a porous conduit with the impact of inclined magnetic field and thermal radiation. The existence of porous material in flow domain creates extra friction, drag, and flow resistance between the flow regime and porous solid surfaces. Considerable attention must be paid to this research work because of its enormous advantages in the industrial manufacturing process, modern technological systems, and many engineering procedures which involve the flow of non-miscible fluid and convective heat transfer process. In this study, the closed-form solutions for Bejan number distribution, entropy production characteristics, flow velocity, and thermal profile are carried out when the two-layered non-miscible fluid is flowing through a rectangular porous conduit. Detailed graphical analysis of the influence of optimal design parameters on the dimensionless velocity distribution, Bejan number distribution, temperature distribution, and entropy production characteristics across the porous conduit have been discussed.

To achieve the objective of the considered problem, the ranges of various design thermal and flow parameters which produces the significant results of this study are considered from past published research articles [6,41,42,44,46]. As mentioned above, the independent design parameters involved in this study are: pressure gradient $P = \frac{dp}{dx}$ lies in the ranges $(-\infty, 0)$ [42], non-dimensional micropolarity parameter α lies between $[0, \infty)$ [44], non-dimensional Hartmann number *Ha* have ranges $[0, \infty)$ [44]. The range of inclination angle parameter λ lies between zero to $\frac{\pi}{2}$ [58]. The non-dimensional parameter *L* lies in the interval $[0, \infty)$ [7]. The permeability of upper and bottom porous region of the flow conduit are assumed as K_1 and K_2 respectively and range of these parameters are taken from the article of [23]. The naturally occurring porous material takes the values less than 0.6 whereas man-made porous substances assumed the porosity value closed to 1 [25]. The contribution of radiative thermal exchange in the flow domain is depicted by term *Nr* which lies in the interval $(0, \infty)$ [41].

5.1. Micropolarity parameter effect on flow properties

Here, we discuss the detailed graphical explanation of micropolarity parameter on Bejan number distribution, flow velocity, temperature profile, and entropy production characteristics. In Figures 2–6, the dotted curves and solid curves depict the impact of micropolarity parameter on various flow properties of non-miscible type of micropolar and Newtonian fluid for man-made porous material and naturally occurring porous materials respectively. Figures 2 and 3 visualize the distributions of micropolarity parameters on angular and linear flow characteristics of two-layered non-miscible micropolar and Newtonian fluid in a rectangular flow conduit respectively. The angular flow velocity (microrotation) of micropolar fluid particles decelerates with the ascending trend of micropolarity parameter α, as displayed in Figure 2. Figure 2 demonstrates that the microrotation decreases slowly till the middle of the micropolar fluid region and then it decreases rapidly towards the upper porous boundary of the channel and tends to zero which verifies the no-spin boundary conditions at the upper porous wall of the flow conduit. Figure 3 illustrates that, with an enhancement in micropolarity parameter, there is high deceleration in the flow velocity of non-miscible fluid throughout the porous duct. The physics behind this is the characteristics property of micropolar fluid. The characteristics property of micropolar fluid is that the fluid particles rotate about its own axis with high angular velocities and hence a large amount of momentum of fluid particles transferred to the rotational motion of the fluid particles. Due to this reason, the linear flow velocity of non-miscible nature of micropolar and Newtonian fluid decreases. It can be noticed that the peak value of velocity distribution for small values of micropolarity parameter is observed in porous–porous interface, however, for larger value of micropolarity parameter, the peak value of velocity distribution shifted towards the Newtonian fluid region. Such results are validated with the article published by Murthy and Srinivas [42]. Figure 4 illustrates the evolution in temperature distribution profile of two-layered non-miscible fluid flow through porous duct with the decreasing trend of micropolarity parameters. This result occurs due to the presence of micropolarity parameter in micropolar fluid which reduces the linear motion of fluid in the porous conduit and hence the dissipation of energy reduces and consequently the thermal profile of non-miscible fluid decreases in porous flow channel. The behavior of entropy production characteristics with ascending trend of micropolarity parameter is portrayed in Figure 5.

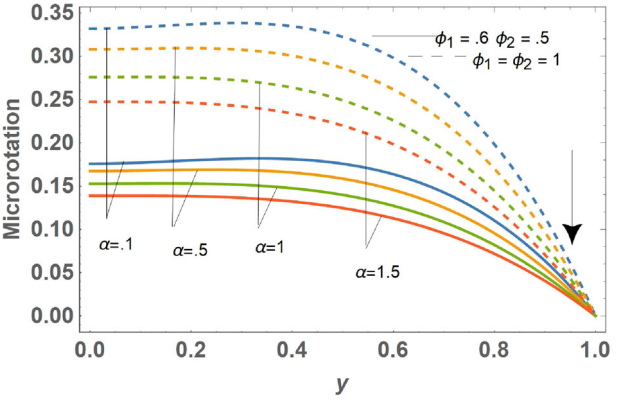

Figure 2. Behavior of microrotational velocity ω via micropolarity parameter α, when $P = -1.5$, $Da = 0.1, L = 1, n_K = 1.2, Ha = 0.5, Br = 0.5, \delta = 0.7, Re = 2.5, \Omega = 1, n_\mu = 0.9, n_k = 1.1, \lambda = 0.5$, $n_\sigma = 0.5, Nr = 1$.

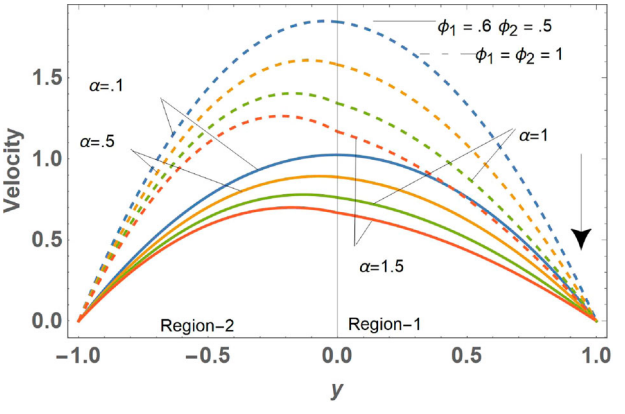

Figure 3. Behavior of velocity profile via micropolarity parameter α, when $P = -1.5, Da = 0.1, L = 1, n_K = 1.2, Ha = 0.5, Br = 0.5, \delta = 0.7, Re = 2, \Omega = 1, n_\mu = 0.9, n_k = 1.1, \lambda = 0.5, n_\sigma = 0.5, Nr = 1$.

The given figure demonstrates that the nature of entropy production is in descending order with the ascending trend of micropolarity parameter. The production of entropy is lowest at the central zone of the porous flow conduit. The most remarkable result which emerges from the current discussion is that the production of entropy for immiscible fluid attains its extremum value in Newtonian fluid region. The science behind this fact is that the Newtonian fluid viscosity in the bottom porous layer is higher as compared to micropolar fluid in the upper porous layer. Figure 6 visualizes the nature of the Bejan number distribution with estimated values of the micropolarity parameter. The Bejan number distribution of non-miscible fluid in porous flow channel rises with the ascending trend of micropolarity parameter. These results are approved with the articles published by Srinivas et al. [42,43].

5.2. Hartmann number effect on flow properties

The comparative study of various flow and thermal properties like entropy production characteristics, Bejan number distribution, flow velocity and thermal field of two-layered

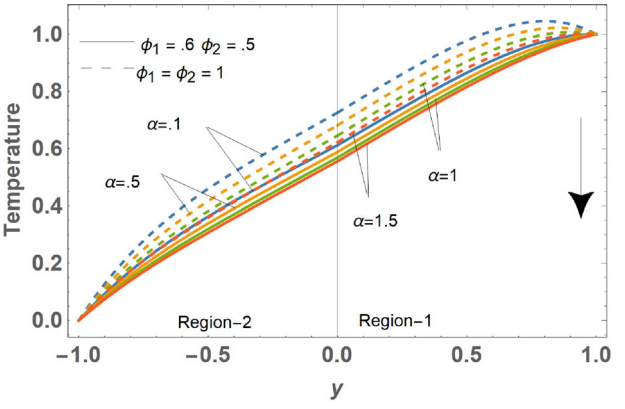

Figure 4. Behavior of temperature profile via micropolarity parameter α, when $P = -1.5, Da = 0.1, L = 1, n_K = 1.2, Ha = 0.5, Br = 0.5, \delta = 0.7, Re = 2.5, \Omega = 1, n_\mu = 0.9, n_k = 1.1, \lambda = 0.5, n_\sigma = 0.5, Nr = 1$.

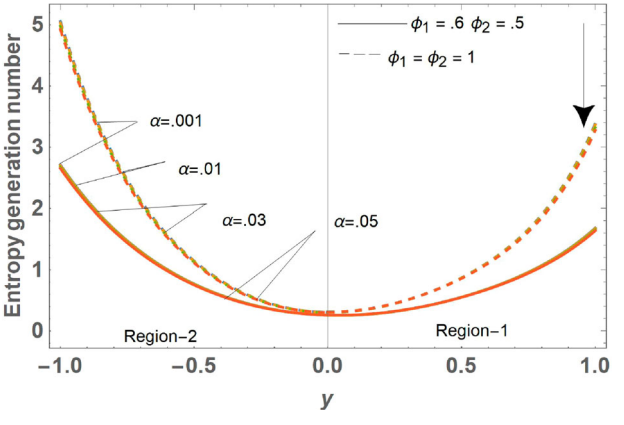

Figure 5. Behavior of entropy generation number via micropolarity parameter α, when $P = -1.5, Ha = 0.5, Br = 0.5, \delta = 0.7, Re = 2.5, \Omega = 1, n_\mu = 1, n_k = 1, \lambda = 0.5, n_\sigma = 1, n_K = 1, L = 1, Da = 0.1$.

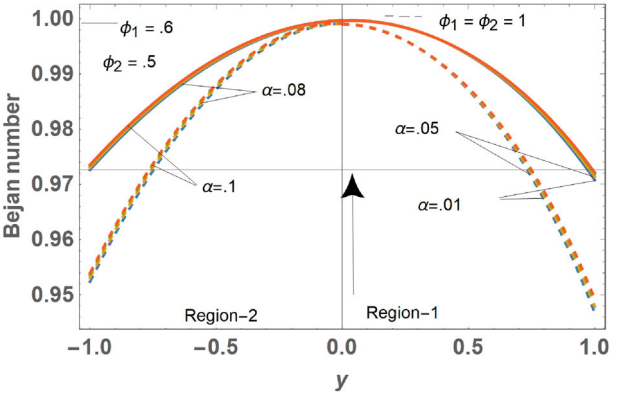

Figure 6. Behavior of Bejan number via micropolarity parameter α, when $P = -0.1, Ha = 0.5, Br = 0.5, \delta = 0.7, Re = 2.5, \Omega = 1, n_\mu = 1, n_k = 1, \lambda = 0.5, n_\sigma = 1, n_K = 1, L = 1, Da = 0.1$.

non-miscible fluid within a porous conduit with various estimated values of Hartmann number is presented in this section. Figure 7 shows the variation of flow velocity with estimated ranges of Hartmann number. From this figure, it is observed that continuous growth in the Hartmann number profile diminishes the flow velocity of two non-miscible micropolar and Newtonian fluid in a porous flow domain. The science behind this fact is the existence of strong magnetic field in the flow domain which develops the Lorentzian magnetic drag force in the flow field of immiscible fluid. Consequently, this drag force decelerated the non-miscible fluid motion in both the regions of the duct. The behavior of the Hartmann number on microrotational velocity is displayed in Figure 8. It shows that, with the ascending trend in Hartmann number profile, the microrotational velocity of micropolar fluid decreases in upper porous zone. Figure 9 shows the influence of Hartmann number on the thermal profile of non-miscible fluid within a rectangular porous channel. This figure presents that temperature profile in more than half of the Newtonian and micropolar fluid region towards the wall of the conduit reduces on rising the strength of the applied magnetic field. An important conclusion is made from this figure that the temperature profile in naturally occurring porous medium nearby the interface enhancing on increasing the Hartmann number. Temperature profile reduces for larger values of Hartmann number and peak value of temperature profile is obtained in the micropolar fluid zone. This result is verified with the previously published articles [42,46]. The Hartmann number impact on entropy production distribution is disclosed in Figure 10. Rising Hartmann number causes the reduction in entropy generation number of micropolar and Newtonian fluid in more than half of the Newtonian and micropolar fluid region towards the wall of the conduit, however, magnetic field show reverse impact on the entropy generation number nearby the interfacial region. The minimum values of entropy production are noticed in the central zone of the porous domain whereas the extremum values are remarked in the Newtonian fluid region. Physics behind the above result is that, more viscous fluid improves the entropy production in the porous conduits that is why the production of entropy is higher in the Newtonian fluid region. The present results are verified with the references Jangili et al. [44], Nezhad and Shahri [46]. Impact of Hartmann number on Bejan number distribution is displayed in Figure 11. From this figure, an increment in the distribution of Bejan number profile is noticed for ascending values of the Hartmann number. This result has excellent agreement with [44].

5.3. Permeability parameter effect on flow properties

Figure 12 is designed to analyze the permeability parameter impact on the flow distribution of two-layered non-miscible micropolar and Newtonian fluid in the porous conduit. The flow velocity of immiscible fluid shows decreasing trend with the ascending values of permeability parameter. Figure 13 presents the outcomes of permeability parameter on microrotational velocity of two-phase micropolar and Newtonian fluid flow within the porous conduit. It is observed that, for increasing values of permeability parameter, the angular velocity gets decreased within the upper porous domain of the channel. This pattern of plots is observed in the work of Yadav et al. [6,13]. An important finding is observed from Figures 12 and 13 that the flow velocity of non-miscible fluids in naturally occurring porous material is less than as compared to man-made porous material. The physics behind this is the existence of maximum number of solid pores in natural porous material which

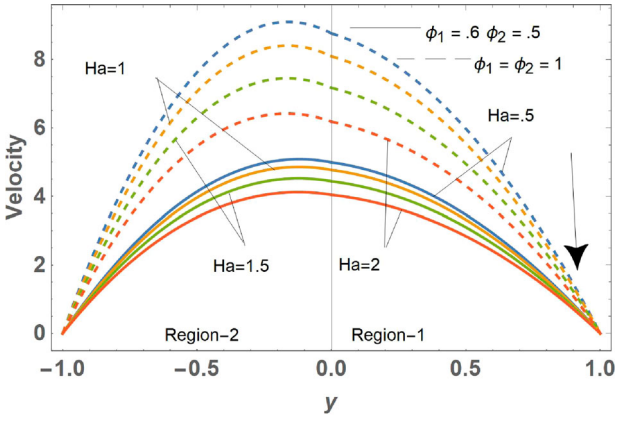

Figure 7. Variation of velocity profile with Hartmann number Ha, when $P = -2, Re = 8, Da = 0.1, L = 1, n_K = 1.2, Br = 0.5, \alpha = 0.2, \delta = 0.7, \Omega = 1, n_\mu = 0.6, n_k = 1.1, \lambda = 0.5, n_\sigma = 0.9$.

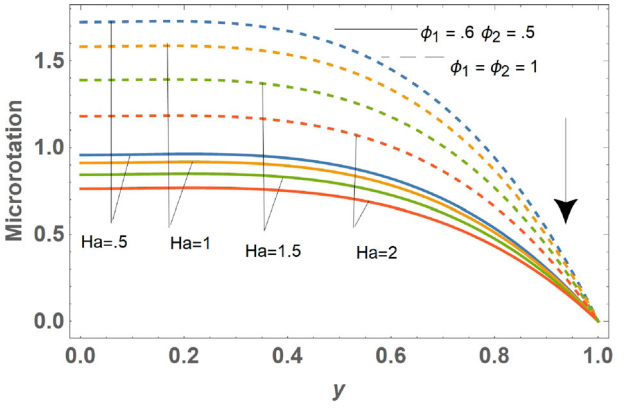

Figure 8. Variation of microrotational velocity ω profile with Hartmann number Ha, when $P = -2, Re = 8, Da = 0.1, L = 1, n_K = 1.2, Br = 0.5, \alpha = 0.2, \delta = 0.7, \Omega = 1, n_\mu = 0.6, n_k = 1.1, \lambda = 0.5, n_\sigma = 0.9$.

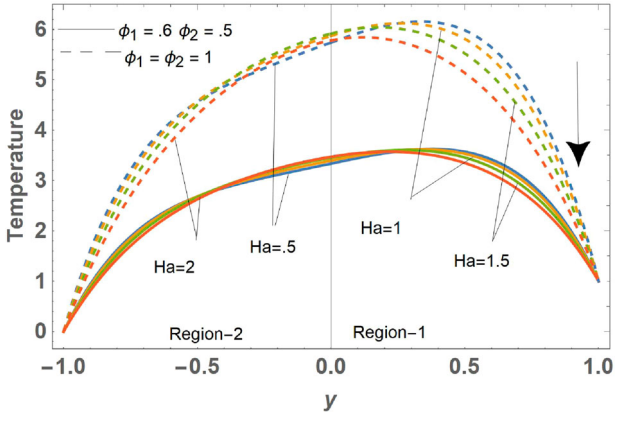

Figure 9. Variation of temperature profile with Hartmann number Ha, when $P = -2, Re = 8, Da = 0.1, L = 1, n_K = 1.2, Br = 0.5, \alpha = 0.2, \delta = 0.7, \Omega = 1, n_\mu = 0.6, n_k = 1.1, \lambda = 0.5, n_\sigma = 0.9$.

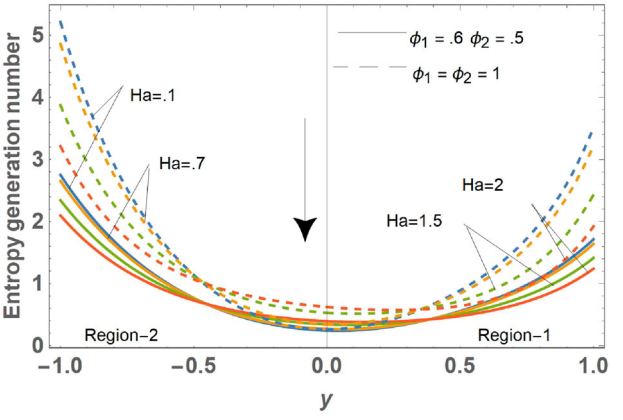

Figure 10. Variation of entropy generation number profile with Hartmann number Ha, when $P = -1.5, Da = 0.1, L = 1, n_K = 1, Re = 2.5, Br = 0.5, \alpha = 0.01, \delta = 0.7, \Omega = 1, n_\mu = 0.9, n_k = 1, \lambda = 0.5, n_\sigma = 1$.

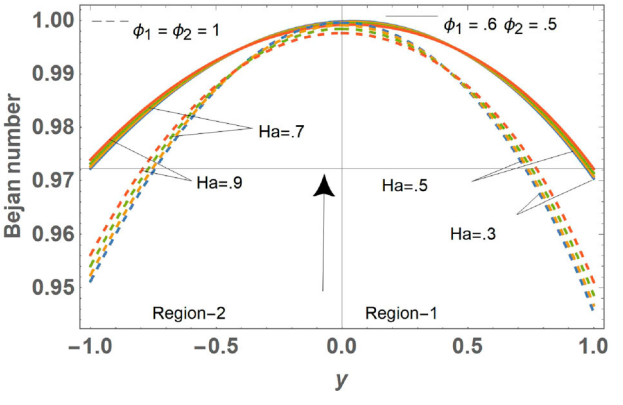

Figure 11. Variation of Bejan number profile with Hartmann number Ha, when $P = -0.1, Da = 0.1, L = 1, n_K = 1, Br = 0.5, \lambda = 0.5, \alpha = 0.01, \delta = 0.7, \Omega = 1, n_\mu = 1, n_k = 1, Re = 2.5, n_\sigma = 1$.

resist the motion of fluid particles in the flow medium. A similar trend of plots is reported by [6]. Figures 14–16 are prepared to analyze the temperature profile, entropy generation number, and on Bejan number respectively. It is concluded from these figures that the permeability parameter shows the same kind of impact on temperature profile, entropy generation number, and on Bejan number respectively as of inclination angle parameter as discussed in the above section. The presence of porous material in the flow domain creates resistance to the motion of the fluid and slows down the flow velocity of immiscible fluid. In this scenario, the conduction is only possible mechanism for heat transfer in flow domain. As a result, the thermal characteristics of non-miscible type of micropolar and Newtonian fluid tends to decrease. Figures 12–14 are in excellent agreement with the findings of references [32]. The temperature profile slightly enhances at the central zone of immiscible fluid for natural porous materials. From Figure 15, it is remarkable that the increasing value of the permeability parameter creates less permeable media which enhances the production of entropy because of friction losses and high pressure drop in the immiscible fluid flow

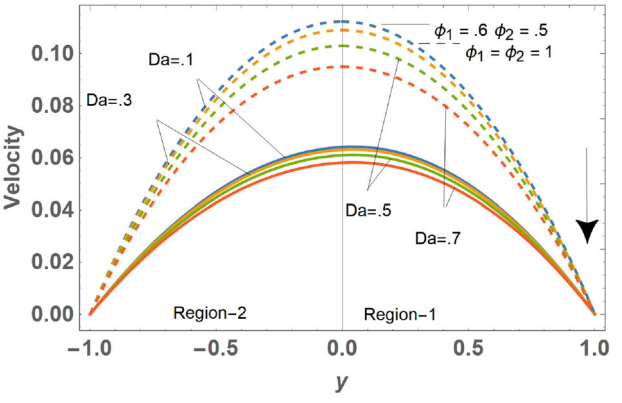

Figure 12. Variation of velocity profile with permeability parameter Da, when $P = -0.1, Ha = 0.5, \lambda = 1, L = 1, n_K = 1, Re = 2.5, Br = 0.5, \alpha = 0.01, \delta = 0.7, \Omega = 1, n_\mu = 1, n_k = 1, n_\sigma = 1$.

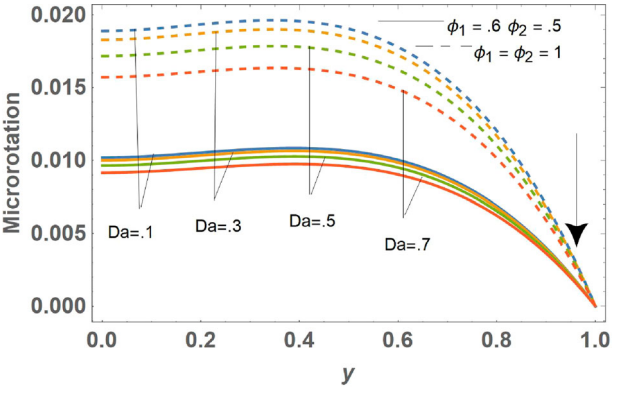

Figure 13. Variation of microrotational velocity ω profile with permeability parameter Da, when $P = -0.1, Ha = 0.5, \lambda = 1, L = 1, n_K = 1, Re = 2.5, Br = 0.5, \alpha = 0.01, \delta = 0.7, \Omega = 1, n_\mu = 1, n_k = 1, n_\sigma = 1$.

domain. Moreover, the entropy production in the porous saturated region is dominated by drag and friction forces between the flow regime and porous solids surface. The distribution of Bejan number slightly increases at the interfacial region of immiscible fluid (Figure 16). Figures 15 and 16 are validated with the findings of references [16,32].

5.4. Radiation parameter effect on flow properties

Entropy analysis, thermal profile, and Bejan number distribution for estimated values of thermal radiation parameter inside a porous flow conduit have been presented in this section. The outcomes of the temperature distribution for the various ranges of radiation parameter are exhibited in Figure 17. This plot concludes that the thermal profile of non-miscible fluid gets reduced by radiation parameter for man-made and natural porous materials both. Figure 18 promulgates that the production of entropy of non-miscible fluid diminishes due to the enlargement of radiation parameter Nr. This figure also concludes that the radiation parameter Nr shows maximum impact nearby the walls of the porous

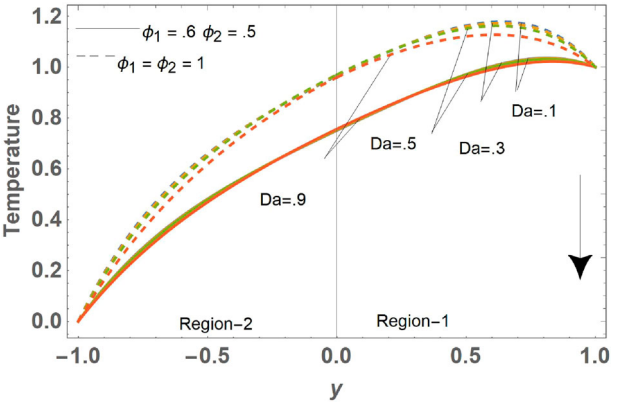

Figure 14. Variation of temperature profile with permeability parameter Da, when $P = -2, Re = 2.5, Ha = 0.5, L = 1, n_K = 1, Br = 0.5, \alpha = 0.01, \delta = 0.7, \Omega = 1, n_\mu = 1, n_k = 1, \lambda = 1, n_\sigma = 1$.

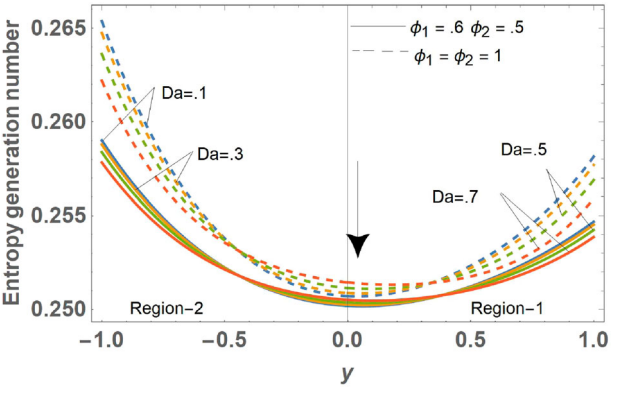

Figure 15. Variation of entropy generation number with permeability parameter Da, when $P = -0.1, Ha = 0.5, \lambda = 1, L = 1, n_K = 1, Re = 2.5, Br = 0.5, \alpha = 0.01, \delta = 0.7, \Omega = 1, n_\mu = 0.9, n_k = 1, n_\sigma = 1$.

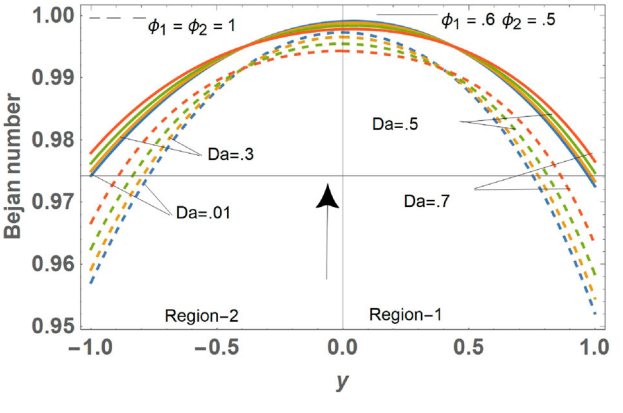

Figure 16. Variation of Bejan number profile with permeability parameter Da, when $P = -0.1, \lambda = 1, L = 1, n_K = 1, Re = 2.5, Br = 0.5, \alpha = 0.01, \delta = 0.7, \Omega = 1, n_\mu = 0.9, n_k = 1, Ha = 0.5, n_\sigma = 1$.

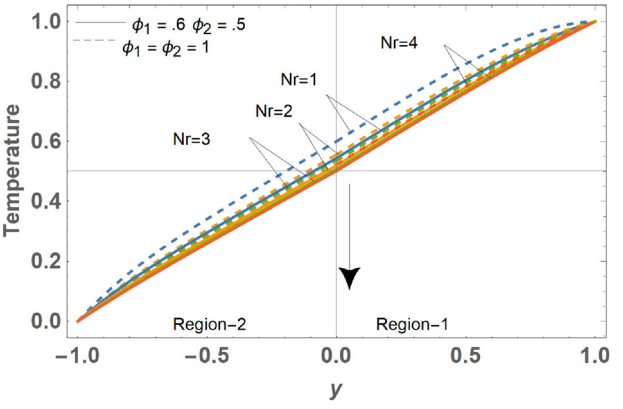

Figure 17. Variation of temperature profile with radiation parameter Nr, when $P = -1.5, L = 1, Da = 0.1, n_K = 1.2, Ha = 0.5, Br = 0.5, \delta = 0.7, \alpha = 2, \Omega = 1, n_\mu = 1, n_k = 1.1, \lambda = 0.5, n_\sigma = 1$.

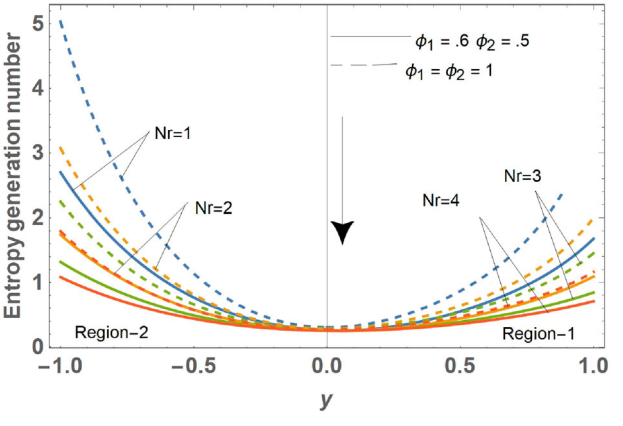

Figure 18. Variation of entropy generation number with radiation parameter Nr, when $P = -1.5, Da = 0.1, L = 1, n_K = 1, Br = 0.5, \lambda = 0.5, \alpha = 0.01, \delta = 0.7, \Omega = 1, n_\mu = 0.9, n_k = 1, Ha = 0.5, n_\sigma = 1, Re = 2.5$.

conduit, however, it shows negligible impact on the entropy generation number at the interfacial region of the non-miscible type of micropolar and Newtonian fluid. It is important to note that the entropy generation number Ns attains its minimum value at the central zone of the conduit whereas the extremum value of entropy arises at the lower porous wall (Newtonian fluid region) of the duct. Figure 19 exhibits the Bejan number Be distribution for various estimations of radiation parameter Nr. This figure presents that the radiation parameter Nr shows the inverse effect on the Bejan number distribution as on the entropy generation number. It is noticed that the distribution of the Bejan number attains its peak value at the central zone of immiscible fluid. These findings are in good agreement with the reference [8].

5.5. Viscous dissipation parameter effect on flow properties

Figures 20 and 21 present the graphical visualization of entropy production number and Bejan number distribution of non-miscible type of micropolar and Newtonian fluid with

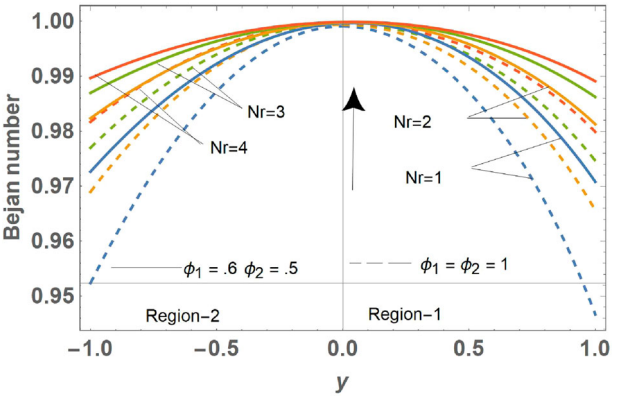

Figure 19. Variation of Bejan number profile with radiation parameter Nr, when $P = -0.1, Da = 0.1, L = 1, n_K = 1, Br = 0.5, \lambda = 0.5, \alpha = 0.01, \delta = 0.7, \Omega = 1, n_\mu = 0.9, n_k = 1, Ha = 0.5, n_\sigma = 1, Re = 2.5$.

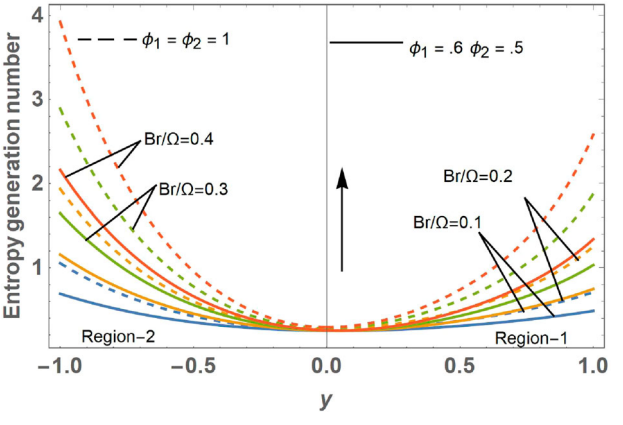

Figure 20. Variation of entropy generation number with viscous dissipation parameter $\frac{Br}{\Omega}$, when $P = -1.5, Da = 0.1, L = 1, n_K = 1, Br = 0.5, \lambda = 0.5, \alpha = 0.01, \delta = 0.7, \Omega = 1, n_\mu = 0.9, n_k = 1, Ha = 0.5, n_\sigma = 1$.

viscous dissipation parameter respectively. It is observed from Figure 20 that an enhancement in viscous dissipation parameter enhances the production of entropy due to increase in fluid friction. It is important to mention that the fluid friction, which enhances on increasing the viscous dissipation parameter, is responsible for the enhancement of production of entropy. From Figure 20, we noticed that the production of entropy is minimum at the central zone of the flow conduit, i.e. useful energy (exergy) is maximum at the interface. These findings are consistent with the work reported by Gorla [49]. The graphical results of Bejan number profile with the viscous dissipation parameter are demonstrated in Figure 21.

5.6. Inclination angle parameter effect on flow properties

In this section, an attempt is made to discuss the influence of inclination angle parameter on flow velocity and entropy generation of non-miscible fluid through man-made and

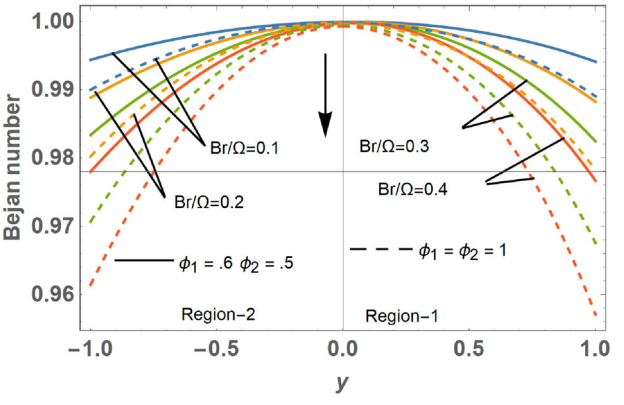

Figure 21. Variation of Bejan number with viscous dissipation parameter $\frac{Br}{\Omega}$, when $P = -1.5, Da = 0.1, L = 1, n_K = 1, Br = 0.5, \lambda = 0.5, \alpha = 0.01, \delta = 0.7, \Omega = 1, n_\mu = 0.9, n_k = 1, Ha = 0.5, n_\sigma = 1$.

naturally occurring porous layered channel. The comparative study of the inclination angle parameter with the flow velocity of the non-miscible fluid in a porous conduit is analyzed in Figure 22. This plot illustrates that by increasing the value of λ, the flow velocity of micropolar and Newtonian fluid shows a continuous decreasing trend in porous channel. The physics behind the above findings is that the Lorentzian magnetic drag force which is produced due to the action of electromagnetic field at an angle $(90 - \theta)$ with the flow direction of the immiscible fluid increases in the opposite direction of the flow and hence the velocity of the fluid decreases. Such graphical results are obtained in the previously published article [14,58]. It is noticed from Figure 22 that the non-miscible fluids achieved higher value in Newtonian fluid region as compared to the incompressible micropolar fluid region. Figure 22 demonstrates that the inclination angle λ show the slightly higher impact on the flow velocity of non-miscible fluid in man-made porous material as comparison to in the naturally occurring porous medium. During the flow analysis of non-miscible fluid, it is observed that the flow velocity of immiscible fluids attains higher values for man-made porous material whose porosity is greater than natural porous material. This result authenticates the fact that the presence of large void spaces in man-made porous material enhances the flow velocity of non-miscible fluid as compared to natural porous material. Figure 23 indicates the impact of λ on entropy generation characteristics of the non-miscible micropolar and Newtonian fluid through a porous duct. As seen in Figure 23, the ascending trend of the inclination angle parameter shows a descending trend of entropy generation number nearby the porous wall of the flow conduit.

The generation of entropy slightly enhances on increasing the inclination angle parameter nearby the central zone of the porous conduit. The production of entropy is higher in the neighborhood of the bottom porous wall of the duct (Newtonian fluid region). The science behind this fact is that the fluid friction irreversibility arises by the Newtonian fluid is more than the micropolar fluid. The higher values of entropy production is noticed for man-made porous material as compared to naturally occurring porous material. Such phenomenon authenticates the fact that the flow velocity of immiscible fluid is higher in man-made porous material because of the presence of large void space in porous substances that is

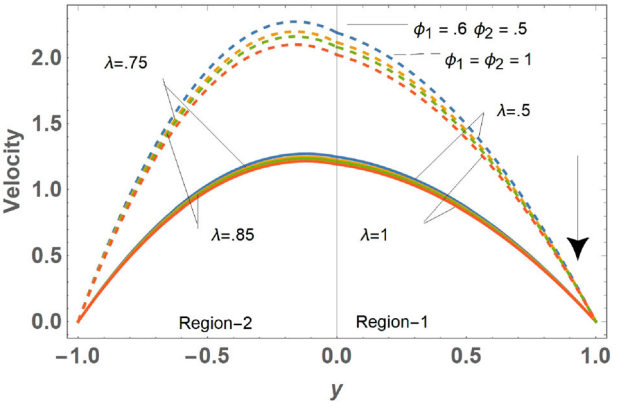

Figure 22. Variation of velocity profile with inclination angle parameter λ, when $P = -2, Ha = 0.5, Da = 0.1, L = 1, n_K = 1.2, Re = 2, Br = 0.5, \alpha = 0.2, \delta = 0.7, \Omega = 1, n_\mu = 0.6, n_k = 1.1, n_\sigma = 0.9$.

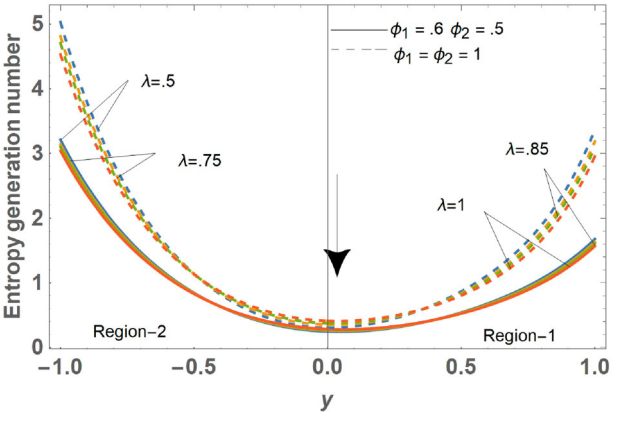

Figure 23. Variation of entropy generation number with inclination angle parameter λ, when $P = -1.5, Da = 0.1, L = 1, n_K = 1, Re = 2.5, Br = 0.5, \alpha = 0.01, \delta = 0.7, \Omega = 1, n_\mu = 0.9, n_k = 1, Ha = 0.5, n_\sigma = 1$.

why the entropy production is maximum in man-made porous medium as compared to naturally occurring porous material.

Table 1 shows the numerical values of temperature and microrotation at the interface of Newtonian and micropolar fluid region of the rectangular porous channel for various values of inclination angle parameter λ. From this table, we concluded that values of temperature at the interfacial region enhance on increasing the inclination angle parameter λ for both types of porous materials, i.e. for naturally occurring as well as man-made porous material. However, the microrotation decreases on enhancing the inclination angle parameter λ.

6. Conclusion

In this work, convective thermal exchange, flow velocity, Bejan number distribution, and entropy production number of the fully developed immiscible micropolar and Newtonian fluid in a rectangular porous enclosure are analyzed. The exergy analysis is performed

Table 1. Numerical values of the temperature and microrotation at $y = 0$ when $P = -0.7, Da = 0.1, L = 1, n_K = 1.2, Br = 0.5, \alpha = 0.2, \delta = 0.7, \Omega = 1, n_\mu = 0.6, n_k = 1.1, Ha = 0.5, n_\sigma = 0.9$.

	Temperature at $y = 0$		Microrotation at $y = 0$	
λ	$\phi_1 = 0.6, \phi_2 = 0.5$	$\phi_1 = 1, \phi_2 = 1$	$\phi_1 = 0.6, \phi_2 = 0.5$	$\phi_1 = 1, \phi_2 = 1$
0.50	3.33537	5.74025	0.239233	0.430819
0.75	3.36269	5.80887	0.234356	0.415418
0.85	3.37513	5.83639	0.231928	0.407917
1.00	3.39444	5.87351	0.227826	0.395481

by using the concept of second law of thermodynamics. In this non-miscible fluid flow problem, we consider the thermal radiation influences together with a constant oriented magnetic field which is functioned perpendicular to the direction of the flow domain. The coupled system of differential equations arising from this study is solved by well-known methods and the expression for thermal transformation, flow distribution of non-miscible fluid is addressed analytically. The characteristics of various emerging thermal and flow parameters on flow variable of non-miscible type of micropolar and Newtonian fluid are pictorially deliberated. The present flow analysis of entropy production of non-miscible micropolar and Newtonian fluid in a porous flow conduit has many potential applications such as cooling of nuclear reactor, filtration processes, industrial manufacturing processes, and so on. The appropriate analysis of entropy production provides the best knowledge of enhancing the efficiency of thermal system, modifying the system design and optimizing the operating conditions in the system. Thus the present discussion is very helpful in various disciplines of science and engineering community because of its enormous roles in heat transfer related areas. Important observations arise from this work are as follows:

(1) The temperature profile, velocity field, and entropy production characteristics reduce for increasing values of micropolarity parameter.
(2) Hartmann number can be used to reduce the velocity field, entropy generation characteristics, and temperature profile of immiscible fluids.
(3) The entropy generation number and temperature distribution of non-miscible fluid are enhanced in parallel with the radiation parameter.
(4) Permeability parameter decreases the velocity field, thermal distribution, and entropy generation characteristics for the present model. The reason behind this is that the porous medium is composed of some void and solid spaces and presence of these solid spaces in the porous media creates resistance in fluid motion and hence flow velocity of immiscible fluid decreases. In this situation, the conduction heat transfer is the only possible mode of heat transfer which diminishes the temperature profile of immiscible fluid. The entropy production in porous media is dominated by drag and friction forces between the flow regime and porous solids surface.
(5) It is concluded that the entropy generation characteristics have extremum value in the region of Newtonian fluid due to more viscous nature of Newtonian fluid.
(6) During the analysis of the result, it is noticed that the production of entropy is lowest at the central zone of non-miscible fluids while the Bejan number attains its peak value at the centerline of the conduit.

(7) During the flow of immiscible fluid in porous flow channel, a crucial result noticed by authors that all flow variables such as Bejan number distribution, flow distribution, thermal profile, and entropy production number achieved higher values for man-made porous material in comparison to naturally occurring porous material.

The present research work can be extended for entropy production analysis in peristaltic transport of immiscible nature of micropolar and Newtonian fluid in a porous saturated channel. The concept of entropy generation analysis can also be used in blood flow through arteries. The considered problem can be extended for variable flow properties such as varying viscosity and varying permeability.

Disclosure statement

No potential conflict of interest was reported by the author(s).

Funding

This research was funded by Princess Nourah bint Abdulrahman University Researchers, Riyadh, Saudi Arabia Supporting Project number (PNURSP2022R154).

ORCID

Pramod Kumar Yadav http://orcid.org/0000-0003-2763-7848

References

[1] Eringen AC. Simple microfluids. Int J Eng Sci. 1964;2(2):205–217.
[2] Eringen AC. Theory of micropolar fluids. J Math Mech. 1966;16:1–18.
[3] Ariman T, Turk MA, Sylvester ND. Microcontinuum fluid mechanics – a review. Int J Eng Sci. 1973;11(8):905–930.
[4] Ariman T, Turk MA, Sylvester ND. Applications of microcontinuum fluid mechanics. Int J Eng Sci. 1974;12(4):273–293.
[5] Lukaszewicz G. Micropolar fluids: theory and application. Boston: Springer Science & Business Media; 1999.
[6] Yadav PK, Verma AK. Analysis of immiscible Newtonian and non-Newtonian micropolar fluid flow through porous cylindrical pipe enclosing a cavity. Eur Phys J Plus. 2020;135(8):1–35.
[7] Khanukaeva DY, Filippov AN, Yadav PK, et al. Creeping flow of micropolar fluid through a swarm of cylindrical cells with porous layer (membrane). J Mol Liq. 2019;294:111558.
[8] Oahimire JI, Olajuwon BI. Effect of hall current and thermal radiation on heat and mass transfer of a chemically reacting mhd flow of a micropolar fluid through a porous medium. J King Saud Univ-Eng Sci. 2014;26(2):112–121.
[9] Srinivasacharya D, Hima Bindu K. Entropy generation in a micropolar fluid flow through an inclined channel. Alex Eng J. 2016;55(2):973–982.
[10] Ahmed SE, Rashad AM. Natural convection of micropolar nanofluids in a rectangular enclosure saturated with anisotropic porous media. J Porous Media. 2016;19(8):737–750.
[11] Jena SK, Mathur MN. Similarity solutions for laminar free convection flow of a thermomicropolar fluid past a non-isothermal vertical flat plate. Int J Eng Sci. 1981;19(11):1431–1439.
[12] Bhattacharyya K, Mukhopadhyay S, Layek GC, et al. Effects of thermal radiation on micropolar fluid flow and heat transfer over a porous shrinking sheet. Int J Heat Mass Transfer. 2012;55(11–12):2945–2952.
[13] Yadav PK, Jaiswal S. Influence of an inclined magnetic field on the Poiseuille flow of immiscible micropolar–Newtonian fluids in a porous medium. Can J Phys. 2018;96(9):1016–1028.

[14] Nikodijevic D, Stamenkovic Z, Milenkovic D, et al. Flow and heat transfer of two immiscible fluids in the presence of uniform inclined magnetic field. Math Probl Eng. 2011;2011(3):1–18.
[15] Srivastava BG, Deo S. Effect of magnetic field on the viscous fluid flow in a channel filled with porous medium of variable permeability. App Math Comp. 2013;219(17):8959–8964.
[16] Komurgoz G, Arikoglu A, Ozkol I. Analysis of the magnetic effect on entropy generation in an inclined channel partially filled with a porous medium. Num Heat Transfer. 2012;61(10):786–799.
[17] Sharma BD, Yadav PK. A mathematical model of blood flow in narrow blood vessels in presence of magnetic field. Natl Acad Sci Lett. 2019;42(3):239–243.
[18] Bhatti MM, Abdelsalam SI. Bio-inspired peristaltic propulsion of hybrid nanofluid flow with Tantalum (Ta) and Gold (Au) nanoparticles under magnetic effects. Waves Random Complex Media. 2021;1–26. DOI:10.1080/17455030.2021.1998728.
[19] Shahid A, Bhatti MM, Ellahi R, et al. Numerical experiment to examine activation energy and bi-convection Carreau nanofluid flow on an upper paraboloid porous surface: application in solar energy. Sustain Energy Technol Assess. 2022;52:102029.
[20] Bhatti MM, Abbas T, Rashidi MM, et al. Numerical simulation of entropy generation with thermal radiation on MHD Carreau nanofluid towards a shrinking sheet. Entropy. 2016;18(6):200.
[21] Rashidi MM, Bhatti MM, Abbas MA, et al. Entropy generation on MHD blood flow of nanofluid due to peristaltic waves. Entropy. 2016;18(4):117.
[22] Darcy H. Les fontaines publiques de la ville de Dijon. Paris: Dalmont; 1856.
[23] Brinkman HC. A calculation of the viscous force exerted by a flowing fluid on a dense swarm of particles. Flow Turbul Combust. 1949;1(1):27–34.
[24] Bejan A. Convection heat transfer. New Jersey: John Wiley and Sons; 2013.
[25] Nield DA, Bejan A. Convection in porous media. New York: Springer; 2006.
[26] Vafai K, Tien CL. Boundary and inertia effects on flow and heat transfer in porous media. Int J Heat Mass Transfer. 1981;24(2):195–203.
[27] Kaviany M. Principles of heat transfer in porous media. New York: Springer Science and Business Media; 2012.
[28] Rudraiah N, Nagaraj ST. Natural convection through vertical porous stratum. Int J Eng Sci. 1977;15(9–10):589–600.
[29] Kaviany M. Laminar flow through a porous channel bounded by isothermal parallel plates. Int J Heat Mass Transfer. 1985;28(4):851–858.
[30] Umavathi JC, Chamkha AJ, Mateen A, et al. Unsteady oscillatory flow and heat transfer in a horizontal composite porous medium channel. Nonlinear Anal: Model Control. 2009;14(3):397–415.
[31] Chamkha AJ. Flow of two-immiscible fluids in porous and nonporous channels. J Fluids Eng. 2000;122(1):117–124.
[32] Morosuk TV. Entropy generation in conduits filled with porous medium totally and partially. Int J Heat Mass Transfer. 2005;48(12):2548–2560.
[33] Ansari IA, Deo S. Effect of magnetic field on the two immiscible viscous fluids flow in a channel filled with porous medium. Natl Acad Sci Lett. 2017;40(3):211–214.
[34] Deo S, Maurya DK, Filippov AN. Influence of magnetic field on micropolar fluid flow in a cylindrical tube enclosing an impermeable core coated with porous layer. Colloid J. 2020;82(6):649–660.
[35] Maurya DK, Deo S, Khanukaeva DY. Analysis of Stokes flow of micropolar fluid through a porous cylinder. Math Methods Appl Sci. 2021;44(8):6647–6665.
[36] Bhatti MM, Abdelsalam S. Thermodynamic entropy of a magnetized Ree–Eyring particle-fluid motion with irreversibility process: a mathematical paradigm. J Appl Math Mech. 2021;101(6):e202000186.
[37] Bejan A. Entropy generation minimization. Boca Raton, FL: CRC Press; 1996.
[38] Magie WF . The second law of thermodynamics. New York: Harper and Brothers Publishers; 1899.
[39] Bejan A. Second law analysis in heat transfer. Energy. 1980;5(8–9):720–732.
[40] Bejan A. A study of entropy generation in fundamental convective heat transfer. J Heat Transfer. 1979;101(4):718–725.
[41] Jangili S, Adesanya SO, Falade JA, et al. Entropy generation analysis for a radiative micropolar fluid flow through a vertical channel saturated with non-Darcian porous medium. Int J Appl Comput Math. 2017;3(4):3759–3782.

[42] Murthy JVR, Srinivas J. Second law analysis for Poiseuille flow of immiscible micropolar fluids in a channel. Int J Heat Mass Transfer. 2013;65:254–264.
[43] Muthuraj R, Srinivas S. Fully developed MHD flow of a micropolar and viscous fluids in a vertical porous space using ham. Int J Appl Math Mech. 2010;6(11):55–78.
[44] Jangili S, Murthy JV. Thermodynamic analysis for the MHD flow of two immiscible micropolar fluids between two parallel plates. Front Heat Mass Transfer. 2015;6(1):1–11.
[45] Srinivas J, Murthy JVR, Chamkha AJ. Analysis of entropy generation in an inclined channel flow containing two immiscible micropolar fluids using ham. Int J Numer Meth Heat Fluid Flow. 2016;26(3/4):1027–1049.
[46] Nezhad AH, Shahri MF. Entropy generation case studies of two-immiscible fluids under the influence of a uniform magnetic field in an inclind channel. J Mech. 2016;32(6):749–757.
[47] Mahmud S, Fraser RA. Flow, thermal, and entropy generation characteristics inside a porous channel with viscous dissipation. Int J Therm Sci. 2005;44(1):21–32.
[48] Chauhan DS, Kumar V. Effects of slip conditions on forced convection and entropy generation in a circular channel occupied by a highly porous medium: Darcy extended Brinkman–Forchheimer model. Turk J Eng Env Sci. 2010;33(2):91–104.
[49] Gorla RSR. Second law analysis of mixed convection in a laminar. Non-Newtonian fluid flow through a vertical channel. Int Sch Res Notices. 2011;2011:1–13.
[50] Paoletti S, Rispoli F, Sciubba E. Calculation of exergetic losses in compact heat exchanger passages. Am Soc Mech Eng Adv Energy Syst. 1989;10:21–29.
[51] Abbas MA, Bai Y, Rashidi MM, et al. Analysis of entropy generation in the flow of peristaltic nanofluids in channels with compliant walls. Entropy. 2016;18(3):90.
[52] Bhatti MM, Abbas T, Rashidi MM, et al. Entropy generation on MHD Eyring–Powell nanofluid through a permeable stretching surface. Entropy. 2016;18(6):224.
[53] Qing J, Bhatti MM, Abbas MA, et al. Entropy generation on MHD Casson nanofluid flow over a porous stretching/shrinking surface. Entropy. 2016;18(4):123.
[54] Riaz A, Bhatti MM, Ellahi R, et al. Mathematical analysis on an asymmetrical wavy motion of blood under the influence entropy generation with convective boundary conditions. Symmetry. 2020;12(1):102.
[55] Straughan B. Stability and wave motion in porous media. New York: Springer Science and Business Media; 2008.
[56] Happel J, Brenner H. Low Reynolds number hydrodynamics: with special applications to particulate media. The Hague: Martinus Nijhoff Publishers; 1983.
[57] Ochoa-Tapia JA, Whitaker S. Momentum transfer at the boundary between a porous medium and a homogeneous fluid–II. Comparison with experiment. Int J Heat Mass Transfer. 1995;38(14):2647–2655.
[58] Nikodijevic D, Milenkovic D, Stamenkovic Z. MHD Couette two-fluid flow and heat transfer in presence of uniform inclined magnetic field. Heat Mass Transfer. 2011;47(12):1525–1535.
[59] Khanukaeva DY, Filippov AN, Yadav PK, et al. Creeping flow of micropolar fluid through a swarm of cylindrical cells with porous layer (membrane). J Mole Liq. 2019;294:111558.
[60] Ahmadi G. Self-similar solution of incompressible micropolar boundary layer flow over a semi-infinite plate. Int J Eng Sci. 1976;14(7):639–646.